Tribolysis

– *Reaction of Aromatic Halides for Potential Dehalogenation*

Oluwaseunnla P. Adelusi

Mechanical Engineering, master's level (120 credits)
2022

Luleå University of Technology
Department of Engineering Sciences and Mathematics

LULEÅ
UNIVERSITY
OF TECHNOLOGY

Acknowledgement

Abstract

Out of the 17 Sustainable Development Goals (SDGs) adopted by the United Nations in 2015, chemicals and waste management are obtainable under six. Improper and unsafe disposal of toxic chemicals into the environment affects life below water (SDG 14), human health and well-being (SDG 7), and clean water and sanitation (SDG 6). The twelfth Sustainable Development Goal (SDG 12) focuses on chemical waste management to promote environmental sustainability as a specific target. Thus, in line with creating a safe environment, the last decades have seen the development of technologies and inventions for recycling and safe disposal of chemical wastes. Furthermore, there has been vast adoption of policies in countries worldwide restricting the production and use of toxic chemical wastes such as persistent organic pollutants (POPs). For POPs like Polychlorinated Biphenyls, these policies play a significant role but are howbeit insufficient. The years of production and use of PCBs in the industry before adopting the policies have led to the build-up of large amounts of toxic fluids containing PCBs in storage, awaiting a safe disposal or remediation procedure. Although extensive work has been put into developing PCB remediation methods, most of this has been towards remediating contaminated soil. Therefore, this investigation is focused on a new remediation method for decomposing PCBs in toxic fluid wastes, especially from transformers. Mechanochemical processing has previously been applied for the dehalogenation of POPs. Thus, this study aimed at creating a dehalogenation chemical reaction of aromatic halides with a laboratory tribo-tester. The findings from this research provide valuable information about optimising the tribolysis process towards the development of the tribodevice under TriboREMEDY, a European Union Horizon 2020 project.

Table of contents

List of Tables

List of Figures

Abbreviations

PCB   Polychlorinated biphenyls

POPs   Persistent Organic Pollutants

DCT   3, 4-Dichlorotoluene

SRV   Reciprocating Sliding Friction and Wear Test

FTIR   Fourier-Transform Infrared Spectroscopy

Introduction

Polychlorinated biphenyls (PCBs) are a group of toxic compounds identified as Persistent Organic Pollutants (POPs). POPs, as the name implies, persist for long years and accumulate, a consequence of the physicochemical features of the compounds [1]–[3]. PCBs are combinations of substances formed by the chlorination of biphenyls aided by an appropriate reagent. For years, PCBs have been applied widely in a myriad of manufacturing uses, for example, in the manufacture of transformer fluids, process fluids, capacitors dielectrics, hydraulic solutions and thermal converters lubricants amongst others. The value of PCBs emanates from their physical and chemical stability, combustion resistance, and electrical insulation abilities [1], [4]. In light of the aforementioned definitions, this study covers the review of Polychlorinated Biphenyls (PCBs) literature with specific reference to its history, environmental effects and remediation methods, with emphasis on mechanochemical degradation.

1.1 History of Polychlorinated Biphenyls (PCBs)

Polychlorinated biphenyls (PCBs) form a class of compounds originating between 1930 and 1977. As a result of their thermal and biochemical stability, PCBs were applied for cooling systems and greases in electrical apparatus such as converters for electric equipment. Since PCBs have fireproof abilities, chemical stability, high flash and melting points, and insulating abilities in electrical equipment, they were used in turbines, thrusts greases, and cutting lubricants for metal work and also used as plasticizers, varnishes, glues, insecticides, toners, colours and polishes [4], [7].
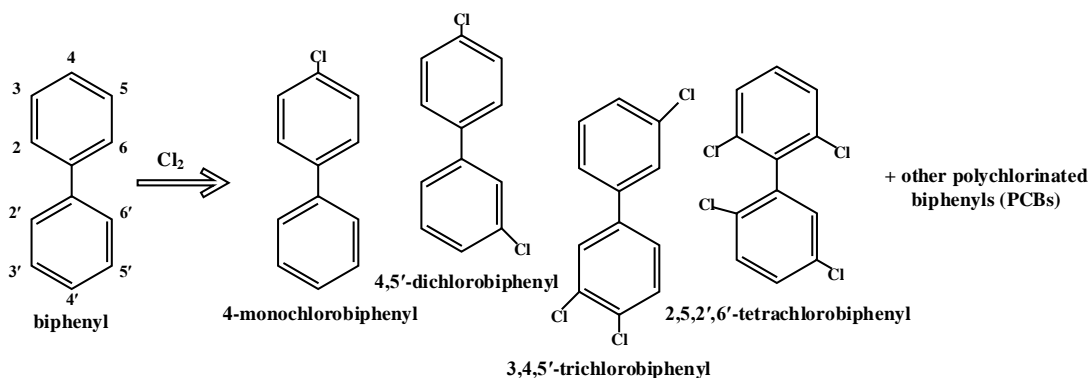
Figure 1: Production of PCBs by direct chlorination of biphenyl [8], [9]

PCBs were made as a combination of PCB congeners going in various terms, for instance, the famous Aroclor used in manufacturing industries was made in various mixtures [10]. A PCB is made up of benzene rings connected to each other and to chlorine atoms. These chlorine atoms attach to the benzene rings in different positions which result in a variety of PCB congeners [11], [12]. According to the United States Environmental Protection Agency, there are 209 PCB congeners in existence varying in the arrangement and number of chlorine atoms in the PCB molecule [7]. PCB congeners vary in toxicity level due to the correlation between chemical structure and toxicity in PCBs. Although all PCB mixtures contain about 175 types of congeners, commercial mixtures were processed with large contents of heavily chlorinated congeners such as Aroclors 1242, 1248, 1254, and 1260 [7], [13]. The congeners were usually mixed in varying ways to influence the bulk properties of the compounds produced. The viscosity of the PCBs increases with chlorination level implying that the oily liquids have lesser chlorine atoms. At low temperatures, it transforms into solid resins [14]. Since 1977, the US banned the production of PCBs in the realization that their build-up and tenacity were harmful to animals, plants, and humans. To date, there is no evidence of products and equipment in the market that contain traces of PCBs in the US; nonetheless, there is the possibility that some unrelated industrial productions discharge some traces of PCBs [10].

1.2 The Nature of PCBs and The Environmental Effects

PCBs are recognized human and environmental threats. As soon as PCB compounds are discharged into the environment, various chemical changes occur in them that become fatal to living things [7], [15], [16]. These chemical changes rely on the degree-level of chlorination of the biphenyl particles [10], [16]. PCB congeners with high chlorination have high octanol-water partition coefficients which explain their presence in soil and sediments. These PCBs sip intensely to soil deposits, and they endure, having long periods of half-lives. Furthermore, PCBs also bio-accumulate in the food cycles and fatty tissues due to their chemical stability. The contamination is widespread as PCBs partition to sediments between aquatic and solid phases resulting from the low solubility in water and vapour pressure [17], [18]. This is the primary reason for the biomagnification of PCBs. In water, PCBs are ingested by aquatic animals and get concentrated in a process called bioaccumulation [15]. Bioaccumulation increases the concentration of PCBs from water to organism making the organism's PCB levels about a million times higher. The PCB concentration increases as it transfers from animal to animal in the rising food chain. Although PCB contact

could transpire due to the contact or breathing in contaminated air, foodstuff ingestion is the major source of PCB contact, thereby being hazardous to human health [10], [16]. The following therefore are empirical literature evidencing the human, animal and ecological hazards resulting from PCBs:

1.2.1 Effects on Animals

Jokinen et al. assessed the dangers of prolonged contact with dioxin (2,3,7,8 tetrachlorodibenzo-p-dioxin, TCDD) and chlorinated biphenyl (3,30,4,40,5 pentachlorobiphenyl, PCB 126) on the cardiac structure in feminine Harlan Sprague Dawley rats. The findings revealed that the mice's cardiac structures were affected by dioxin and PCB 126 [19]. This was shown by the upsurge of impulsive heart failure and inflammation of the heart arteries in the mice. Furthermore, studies by Lind et al. indicated that contact of female mice with PCBs caused amplified rates of antitoxin-saturated fatty acid, amplified blood compression, and an upsurge of arteriole magnitude [20].

1.2.2 Effects on Human Health

The hazardous nature of PCBs means that their effects on the human body can take a myriad of manifestations, some of which are described below.

Diabetes Mellitus and Low Immunity

Rylander et al. tested serum PCB 153 accumulations in Swedish fishers and their spouses. The respondents, averaging 60-64 years, shared about the occurrences of diabetes illness. The experiment expressively indicated that PCB contact and PCB 153 accumulation in the body was likely to cause type II diabetes mellitus [21]. Similar results were shown in a study by Chen et al. and Codru et al. Lee et al. also described comparable conclusions of diabetes occurrence resulting from an accumulation of six selected types of POPs [24]–[26]. In a different experiment, Heilmann et al. inferred the possibility of low immunity among children who ingested PCB. The study revealed that postnatal contact exposure to PCBs affects disease resistance to children's immunization. The experiment tested antibiotics for immunoglobulin reactions over diphtheria and tetanus inoculations for 129 seven-year-old children and 119 children aged 18 months. The immunoglobulin reaction to the diphtheria vaccine diminished by 24.4 % in 18 months olds exposed to PCB. The tetanus inoculation declined by 16.5% for seven-year-old children [27].

Cancerous Diseases

Lindell et al. conducted a study in the United States on the likelihood of PCBs increasing the danger of contracting cancers of lymphocytes. The study showed

that certain PCB compounds, predominantly the advanced chlorinated PCBs (PCB 156, 180, and 194), were linked to augmented danger of contracting cancers of lymphocytes [14], [28]. A study by Hardell et al. in 2004 showed that the accumulation of PCBs in the blood was more significant in victims with testicular cancer, unlike the controls in their population sample. The results augmented the concerns about PCB contamination influencing testicular cancer in unborn male children [29]. Meanwhile, in a 2006 study, Hardell et al. described a link between toxic PCBs on prostate cancer [30]. They compared this to related experiments, establishing PCB exposure as an upsurge factor for contracting prostate cancer. Furthermore, Zani et al. conducted an epidemiological assessment which revealed a relationship between PCB exposure and non-Hodgkin lymphomas [31].

Dermal and Ocular Effects

A report by ATSDR indicated that skin problems such as irascibility, radish skin disease, and colouring of nails and skin have been witnessed from people who accidentally ingested rice and oil contaminated with PCBs in the course of the Yusho and Yu-Cheng poisoning cases [15]. The cutaneous side effects reported in employees presented in seditious folliculitis due to PCBs contact. Palpable side effects, such as hypersecretion of the Meibomian glands and unusual colouration of the eyes, have been reported due to PCB poisoning. These palpable changes certainly escort skin problems. Enduring lengthy ingestion of PCBs in primates resulted in adversative cutaneous and palpable side effects even from dose rates as little as 0.005 mg/kg per day.

Biological and Reproduction Effects

A study by Natalia et al. indicated a relation between early menopause and ecological contact to exposure to POPs including PCB−70, −99, −105, −118, −138, −153, −156, −170, and −183. In their study of Endocrine-disrupting chemicals (EDCs), they showed that victims had six times the probability of having early menopause [32]. Buck Louis et al. investigated fecundity, the physiological potential to bear children, of couples exposed to POPs including 36 PCB groups. PCB was associated with up to 29% reduction in fecundity in males and 21% in females [33]. In addition, Denham et al. established that PCB congeners influenced the early attainment of menarche in young girls who were exposed to PCB in Akwesasne Mohawk Nation [34].

Neurological Effects

A 2017 study by Fimm et al. revealed the effects of PCB exposure on word fluency and sensorimotor processing. The statistics indicated that PCBs cause nerve variations in human offspring from mothers exposed to PCBs from a young

age, although these changes are restrained. In certain experiments, these variations vanished when the children were older than 2-4 years; however various other experiments indicated persistence for over 11-year-olds typically as a result of PCBs contact when they were in the womb. Mothers who ingested PCBs through fish in North Carolina, the Netherlands and Germany, had newborns with neurodevelopmental problems and challenges even in later life. These recollection and intelligence quotient mark shortages were linked to before-birth contact with PCBs through tests done from blood tested from the umbilical string. Experiments on animals also confirmed that PCBs can prompt an adversative nervous alteration in young and mature ones. These symptoms include strange impulses and recollection shortfalls, low ability to learn and challenged intelligence quotients in newborns. The probability of a child exposed to PCBs having a low IQ is three times more, and the child is two times more likely to be at least two years behind in intellectual capacity . The ATSDR report of 2015 duly highlighted studies on humans and animals that revealed nerve distortions resulting from PCB contact [15].

1.2.3 Effects of PCBs on Plants

Anyasi and Atagana evaluated the negative effects of PCBs on plant growth and development in their 2011 study. The evaluation recognized, for instance, algae stunted growth as indicated by algae cell amounts scoring a stumpy rate of 0.3-10 ppm due to PCBs in a waterly mixture [1]. There is also the existence of scarce stunted growth in advanced vegetation due to exposure to PCBs. Strek and Weber indicated deformities on leaves of young soybean budding in soil subjected to 1000 ppm Aroclor-1254 [36]. A decrease in plants' tallness and fresh mass was indicated in soybean, beets and pigweed. At a 1000 ppm rate of Aroclor 1254, soybean growing was subdued by around 47%.

1.3 Historical Overview of PCBs Remediation Methods Up Till 2021

Since the Stockholm Convention in 2004 and the call for the elimination or restriction of the production and use of persistent organic pollutants (POPs), there has also been research aimed at developing techniques to remediate the POPs in the environment, including remediation for Polychlorinated biphenyls (PCBs). Many of these processes are unsustainable because of the energy and cost requirements in addition to the drawbacks of creating toxic byproducts into the environment. Furthermore, most of this research has been concentrated on PCB-contaminated soil with lesser attention on bulk PCB-contaminated fluids such as waste from old transformers.

1.3.1 Oxidation

Oxidation treatment is a basic, although very effective vigorous technology used to redress soil polluted by toxic biological compounds and cyanides. Oxidizing mediators applied in this method encompass a broad variety of ingredients such as hydrogen peroxide, ozone, and potassium permanganate. These substances help in quickening the annihilation of the poisonous biological composites when applied to the soil [30].

1.3.2 Vapour withdrawal

In this method, vacuity blowers are injected into the soil to remove toxic contaminants. The toxic chemicals are then treated at the site using stimulated carbon sifters and stimulant sieves. The efficiency of this method hinges on soil features like water content, warmth and porousness. This technique, however, can be limited by an extraordinarily fine texture of the soil or high soil wetness, thereby affecting the value of soil vapour removal [30].

1.3.3 Phytoremediation

Phytoremediation entails the application of vegetation to dissolve carbon-based toxic compounds such as PCB out of the soil [37]. Harvey et al. described it as a three-in-one process that involved biodegradation of the PCBs in soil, uptake into plant tissues through the roots and finally, transformation into the atmosphere [38]. Tu et al. applied phytoremediation in a soil field and achieved a 78.4% reduction in PCB concentrations within two years of the study [39]. Phytoremediation is one of the suitable techniques in locations with high levels of pollution where alternative remediation methods are uneconomical and in combination with supplementary remediation methods. Deep-seated plants, grasslands, pulses, and marine vegetation are usable in the phytoremediation ground. The method is an operational, unobtrusive, and economical way of remediating soil particles which makes it seen as natural and attractive. It is accepted in affected communities and government authorities as a prospective, well-designed technique especially due to the low cost. In general, it is an environmental-friendly technique as it involves low-tech/energy requirements and has mild environmental impacts [40], [41].

1.3.4 Rhizodegradation Technology

The rhizodegradation technique commonly called "rhizoremediation" is similar to phytoremediation. Both processes are founded on the blend of bacteriological and vegetative growing courses. In rhizodegradation, plant roots activate microbial processes in the soil which lead to biomass build-up, and accordingly, hastens PCB remediation progression [1], [6], [42]. The procedures utilized include land

tillage, injection of substrates to autochthonous microbes, and vegetation growing coupled with a vegetal progression that stimulates rhizobacteria (PGPR). The microbial processes and the extracellular enzymes released from the plant roots act as electron donors in the dehalogenation process [43]. In addition to introducing nutrients into the soil, rhizodegradation has been evidenced to intensify the phytoremediation of Persistent Total Petroleum Hydrocarbons (TPHs) in creosote-polluted topsoil [44].

1.3.5 Chemical Dechlorination

The Amstar dechlorination solution is a chemical degradation method for PCBs. It was developed based on a nucleophilic substitution reaction to eliminate chlorine from PCBs. It specifically worked to prevent the production of by-products that were toxic as well. This technique is known to successfully cleanse steel vessel partitions, soil particles, train track ballast stones and loose lubricants. For partitions with PCB rates bigger than 100 ppm, Amstar reduced PCB contamination as much as from 90 – 99% [45]–[47].

1.3.6 Microbial Degradation of PCBs

This technique is a natural organic practice that uses microbes such as bacteria and fungi to destroy, disrupt, convert and eliminate toxins. There exists evidence of bacteriological remediation of PCBs in aquatic, dry land and other deposits [1], [49]. Bacteriological deprivation of PCBs covers two conceivable paths: anaerobic dehalogenation and aerobic deprivation. Microbial degradation of PCB is done through organohalide inhalation under anaerobic conditions. Meanwhile, organohalide inhalation of PCBs entails an organic method that reduces the toxicity of PCBs through the elimination of chlorines [50], [51].

The PCB congeners act as the electron acceptor with three latent chlorine substitutable spots; para, meta, and ortho [52] and the chlorine atoms are replaced with hydrogen atoms at two principal sites. In their study, Sowers and May indicated two main categories of bioremediation methods, biostimulation and bioaugmentation. The biostimulation technique is used to increase conditions necessary to a contaminated location to catalyze the events of autochthonous microbes. It is performed by 'halopriming', using halogenated mixtures with the capacity to raise the original PCB dechlorinating bacterial reagents and encourage genes essential for dehalogenation [53], [54].

For anaerobic deprivation, biostimulation of native dechlorinating microorganisms is attained through halopriming with benzoates or similar halogenated compounds [53]. In the course of this progression, the chlorine atoms in the PCB compounds are substituted with hydrogen atoms. For years, biostimulation of anaerobic PCB deprivation has been extensively used to remedy

PCB-polluted soil particles and residues; nevertheless, the detailed application remains indistinct. Alternatively, biostimulation is also used for aerobic bioremediation to break low-chlorine PCBs. The backing co-metabolism of PCBs is catalyzed by the application of biphenyl [55].

1.3.7 Bioventing

This is the solitary bioremediation method that permits the handling of diluted soil particles. Although, the method has a shortfall when the water table level is contained by numerous bases from the ground level [56], [57]. This method utilizes a void-boosted soil gas removal structure because of soil compression incline. It results in airflow hooked on the subsurface, thus activating the aerophilic pollutant breakdown course. In some instances, this process entails adding nitrogen salt by scattering a nutrient mixture on the affected soil or by instilling it on the affected soil surface [57]. Adequate airflow is vital in planning a bioventing scheme therefore, it is limited in cases with poor porosity and warmth.
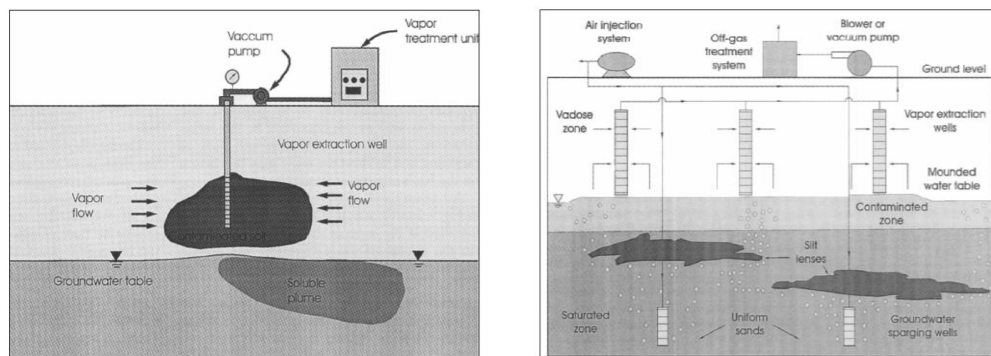
Figure 2: Schematics for (a) Bioventing and (b) Biosparging System [57]

1.3.8 Biosparging

This technique entails a pushing shot of natural oxygen into the contaminated aquifer. It is applied in soaked and unsoaked soil regions. It was premeditated to supplement the inadequacies of the bioventing procedure and thereby lessening energy intake [57]. The administration of atmospheric oxygen into the aquifer causes tiny canals for the oxygen to sip through the unsoaked soil regions. Hence, to create the required plentiful outlets in these passages, the oxygen needs to be throbbed through the soil. Consequently, the pollutants are conveyed to the unsoaked sectors. Finally, a soil gas removal process is utilized to remove the toxic fumes and purify them at the ground level. According to an experimental study done by Gogoi et al. in Damoder valley, Eastern India, biosparging was successful in eliminating 75% of inherent toxins within a year's duration [58]. The efficiency of the technique depends on the hydraulic conductivity being the

same in both the activated zone and its surrounding aquifer. Achieving this is expensive, and increasing the effectiveness of the technique would not be feasible. Hence, the shortcoming of this method is that it is uneconomical despite its success.

1.3.9 Dehalogenation of PCBs by Chemical Reagent

The principle of dehalogenation by organic substances also entails chlorine substitution to produce safer compounds. To achieve termination PCBs, biochemical substances are subjected to great heat and compressions. The biochemical substances commonly applied are magnesium and zinc compounds, low-valent metals, and Fenton's reagent [59]. The initial use of this method dates to ninety years, during which saleable phenols were applied for the dehalogenation of dioxins and furans. Similarly, biochemical substances are applied for the dehalogenation of PCBs to lessen their hazardous nature. When compared with biological remediation methods, PCBs can be effectively degraded quicker and more efficiently in this technique [60], [61].

Mitoma et al. performed an experimental study to detoxicate PCBs using iron-calcium in ethanol at room temperature and pressure under 24 hours. The procedure resulted in a 98% decline in PCB concentration [62]. In a study by Ryoo et al., they performed experiments using aluminium, glycol-600, polyethylene, and potassium hydroxide on PCB-77, 105, 118, 123, and 169. They achieved a PCB elimination of 78% after an experiment of 2 hours at 100°C and a 99% elimination after 4 hours at 150°C [63]. Nah et al. applied ground metal dust, glycol and alkali to eliminate PCBs from used cloistering oil, achieving an elimination effectiveness of 99.9% for the entire PCB mixture [64].

Furthermore, various studies and experiments indicated that a blend of the biochemical mixture and chemical agent for catalytic hydro-dehalogenation could yield a more excellent dechlorination performance [65].

1.3.10 Dehalogenation by Combustion or Incineration

One of the most common methods of waste treatment is combustion and incineration. It entails burning waste at high temperatures (850^0C – 1200^0C) in a controlled environment [66], [67]. High-temperature incineration is mostly applied to soil contaminated with PCBs and has been known to achieve close to 99% removal of toxic compounds. Incinerating liquid PCBs require more technical specifications on the incinerators and reach a higher temperature (1200^0C – 1600^0C) than solids/soil [68], [69]. However, in the process of burning PCBs, they can be transformed into dioxins and furans, compounds with higher

toxicity than PCBs. This, in addition to the high equipment and process costs, makes combustion or incineration a less preferred technique.

1.3.11 Supercritical water oxidation

Supercritical water oxidation applies a system of high temperatures and pressures. In this system, water becomes insoluble while the PCB solubility increases making it degradable. Although the process has been proven to be 99% efficient, it has economic drawbacks. These include the high cost of equipment, equipment maintenance, and the creation of unwanted by-products. The high temperature and pressure systems in this process lead to the production of hydrochloric acid and the accumulation of sticky salts and other solids. These cause corrosion, fouling, plugging, and erosion which requires high costs to prevent [12], [70], [71].

1.3.12 Other Remediation Methods

In addition to the remediation methods listed above, another prominent method is mechanochemical dechlorination which would be described in detail in the next chapter. Other methods include hydrodehalogenation using catalysis in bimetallic systems, ultrasonic radiation, electrokinetic remediation, and nanoscale zero-valent ion-based reductive dehalogenation. Using bimetallic systems catalysis, hydrodehalogenation utilizes reactions within the interface of two metals One metal is the reducing catalyst and has a high reduction potential while the other metal, has a negative reduction potential (zero-valent). During hydrodehalogenation, the zero-valent metal like magnesium corrodes as it reacts with water. This releases hydrogen into the system, and it forms a metal hydride with a reducing catalyst like palladium. Some bimetallic systems include magnesium-palladium, aluminium-palladium, iron-palladium, and iron-nickel. The resulting hydride, PbH_2 causes the dehalogenation of PCBs [72]–[74]. The primary drawback of this process is the possibility of producing toxic by-products. Utilizing metals or metal hydrides for dehalogenation is an aspect that is applied in mechanochemical dechlorination.

Mechanochemical Degradation of Polychlorinated Biphenyls

The background for this form of degradation of polychlorinated biphenyls lies within mechanochemistry or tribochemistry, a term established by G. Heinicke in 1984 [75]. According to the International Union of Pure and Applied Chemistry, IUPAC, mechano-chemical reactions describe all chemical reactions resulting from 'direct mechanical energy absorption''. Kajdas et al. described mechanochemistry as chemical and physical transformations initiated by mechanical energy [76], [77]. Despite being defined in the 90s, there have been mechanochemical experiments dated over centuries. One prominent example is Faraday's experiment of 1820, where he performed the reduction of silver chloride using a simple mortar and pestle to create the mechanochemical reaction [78]. Mechanochemistry can be initiated by several forms of mechanical impact including milling, grinding, and shearing. Since its inception, it has been utilized for different applications including mechanical alloying, synthesis of organic compounds, and environmental remediation [2], [80]–[83].

2.1 Ball Milling and Tribology

Mechanochemistry is influenced by the reactivity of materials. In milling, the material is reduced to smaller-sized particles which implies an increase in the surface area of particles as proven in tribology. In addition, there are changes in structure and composition during the milling process. These changes lead to an increase in surface energy which in turn causes mechano-chemical activation. Stolle et al. described mechanochemistry under three sections including mechanical alloying, mechanical activation, and reactive milling [84]. In environmental remediation, the last two phenomena are seen in effect.

Hence, in this technique, the degradation chemical reaction is stimulated by mechanical energy in the tribo-contact. Typically, PCBs have strong bonds that make require high energy to break down. These bonds can be broken down by a process of mechanochemical activation in a ball mill. The ball milling process creates a tribo-contact as high pressure, friction, shear forces, and surface energy arise within the materials interface .

2.1.1 Milling Energy

In addition to the base metal reactivity, another active role is played by the milling energy. This aspect further proves the mechanical aspect of the mechano-chemical reaction. In tribology, motion is a crucial factor as it leads to friction and wear. Motion within an interface creates a system of energy comparable to the milling process. Predictably, in the case where PCB samples were exposed to magnesium without the milling, no reaction was observed. Despite having significantly small particles and large surface areas, chemical reactions were not initiated with simple hand grinding or stirring. A reasonably high milling energy is required for the nucleophilic substitution of electrons i.e, Cl^- in PCBs being replaced with H^- [87]. Therefore, the milling energy causes rupturing of the strong bonds within the PCBs. Takacs' described this reaction as a 'tribochemical' process with sliding occurring between particles. The equation for the breaking bonds was culled from the Arrhenius equation below [82], [88].

$$k(T) = A \exp\left[- \frac{(E_a - \alpha F)}{(k_B T)}\right]$$ *Equation 1*

Where F is the external mechanical force and α is an appropriate characteristic length.

Degradation of PCBs can be performed in ball mills using lesser energy than several other techniques. The process was patented in 1994 after being applied to wastes containing dichloro-diphenyl-trichloroethane (DDT) and PCB [90].

2.2 The Milling Dehalogenation Principle

Dehalogenation takes place by ball milling the contaminated material with materials that react with the PCBs. Cagnetta et al. classified reagents used in mechanochemical reactions for PCBs into four categories (a) Base metal and metal hydrides, (b) Metal oxides, (c) Neutral species, and (d) Oxidizing agents. Out of these four, the main reagents are the base metals or metal hydrides which replace base metals used with hydrogen donors. These include zero-valent metals, strong electron donors like sodium, magnesium, and aluminium as well as their hydrides. In the majority of cases, metals are used instead of hydrides as they are more cost-effective. Base metals can be used alongside hydrogen donors like alcohol, ether, amines, and amides which prevent the formation of unwanted by-products that could be toxic as well [3], [89], [91]. Additionally, the hydrogen donors increase the reaction rate by forming salts or chlorides with the chlorine given off in the experiments. The chemical reactions are described in equations 2 and 3 with metal and metal hydride respectively.

Toxic PCBs	Base Metal	Ball Milling	HC	Non-toxic products	

$$R-Cl \; + \; Mg \quad + \; 'H' \quad \Rightarrow \quad R-H \; + \; MgCl_2 \qquad \begin{array}{c} \textit{Equation 2} \\ [89] \end{array}$$

Toxic PCBs	Hydride donor	Ball Milling	Hydrocarbon biphenyl	Non-toxic products	

$$C_{12}H_xCl_{12} \; + \; MH \qquad \Rightarrow \qquad E_{um} \, C_{12}H_{10} \; + \; MCl \qquad \begin{array}{c} \textit{Equation 2} \\ [87] \end{array}$$
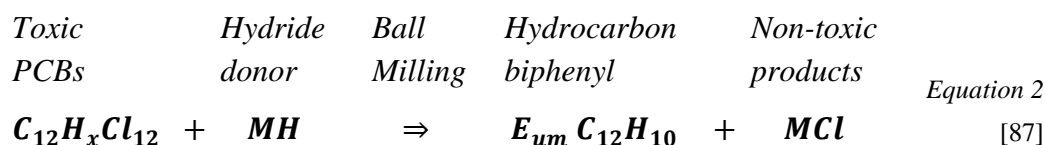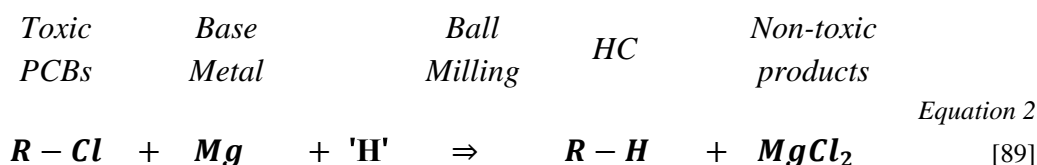
As the mechanical energy causes a breakdown of the C-Cl bonds, the highly reactive base metals react with it to form the parent hydrocarbon biphenyl and magnesium/aluminium chlorides which are safer and non-toxic. The products are seen in the equations above. The process usually entails a single operation in the ball mill reactor under room temperature and pressure and no harmful by-products are produced during or after the ball milling process [89]. A major advantage of the process is its versatility as it is applicable for high and low levels of contamination as well as solids (soils) and liquids (transformer oil).

Aresta et al. conducted high-energy milling experiments using a ring mill made up of a disc and ring for contaminated soil. The experiments showed a 99.99% decrease in PCB concentration in the sand as it reduced from approximately 2600 mg/kg to 0.2 mg/kg [87]. Birke et al. performed similar experiments using centrifugal ball mills and dichlorobenzene (1,3-DCB) as a model substance for PCB [89]. The results showed a complete dichlorination of the sand slurry. While the former used a ternary hydride, Sodium borohydride (NaBH4), Birke et al. performed experiments using magnesium and methanol (hydrogen donor). The chloride formation was inversely proportional to the PCB concentration as shown in figure 3.
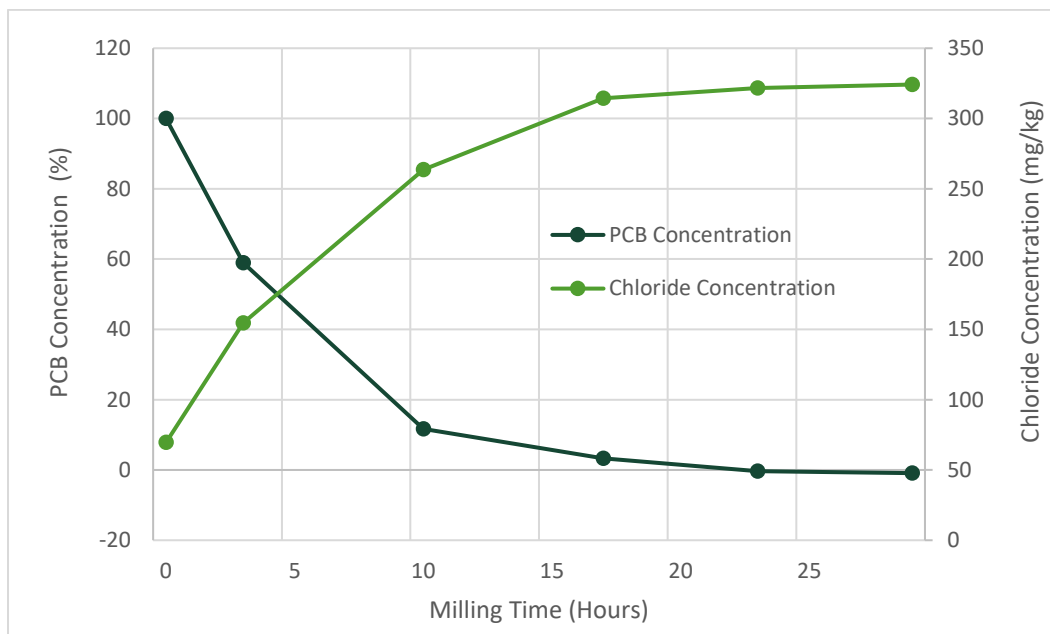
Figure 3: Variation of PCB Concentration in the ball milling process.

In both authors', works and in other literature, Gas chromatography was used for analysis and showed that the level of dehalogenation increases with milling time. Birke et al. realised complete dehalogenation at about 50 minutes compared to 18 hours in the findings of Aresta et al. which is also seen in figure 3. In the works of Nah et al., PCB was removed up to 99.9% within only 2 hours of milling while Wang et al. achieved over 97% PCB removal after four hours of milling with calcium oxide [64], [92]. In general, several experiments have been conducted to show the applicability of mechanochemical reactions for degradation and waste treatment.

The efficiency of PCB removal during these processes can be analysed based on the concentration of PCBs before and after the experiments as described in the equation below.

$$E = 100\% * \left(PCB_{raw\ sample} - PCB_{treated\ sample}\right) \Big/ PCB_{raw\ sample} \qquad Equation\ 3$$

2.2.1 Magnesium in Mechanochemical Degradation of polychlorinated biphenyls

In mechanochemical degradation, the overall reaction time is dependent on the reactivity of the base metal [2], [78]. Hence, for dechlorination to occur successfully in the ball milling process, an excess of base metal is required such that sodium is over seven times the chlorine in the waste or magnesium is sixteen times the chlorine in the waste. Magnesium is preferable despite the excesses

14

because it produces much lesser amounts of phenylcyclohexane, a by-product formed due to further reduction of biphenyl [89], [93]. Furthermore, it has a lower reduction potential than sodium, making it a better electron donor and ultimately a better reactant. Magnesium is also used in this project based on the advantages listed here above.

2.3 Advantage of Mechanochemical Processing for Remediation of PCBs and other POPs

In comparison to the remediation methods listed in the previous chapter, mechanochemical processing has the following benefits [2], [3], [94].

1. The process is simple and usually entails a single operational step. The ball mill is usually a closed reactor, and the process takes place within the device. Therefore, manufacturing and operation are not as complex.
2. Unlike other processes discussed above, mechanochemical processing requires low energy as mechanical energy is the main concern creating no need for thermal energy.
3. The costs for operating the mechanochemical processes are low. Importantly, the process does not require high temperatures as it is a non-combustion technology. Therefore, it eliminates the need for heating and other costs related to manufacturing and maintaining such high-temperature facilities. Furthermore, the reagents are less expensive and easily sourced. Considering the high yield in degradation, compared to the energy input, this process is both cost-efficient and effective.
4. The products from the reaction are non-toxic and safe mineralized compounds, unlike other methods which produce toxic by-products that require further processing. The high degradation efficiency, therefore, makes it a better alternative to several other methods.
5. This process is environmentally friendly as the energy consumption, temperature and pressure requirements are significantly low. Furthermore, it promises sustainability since reactive base metals like magnesium can be obtained from recycled materials.

2.4 Research Gap and Objectives

The call to eliminate persistent organic pollutants at the Stockholm Convention in 2004 led to extensive research being conducted. Some techniques have been developed to remediate the PCBs in the environment, some of which were discussed in the previous sections. However, the study on remediating bulk PCB-contaminated fluid is limited as more focus is on soil remediation. A few of these methods, which are focused on bulk toxic fluids from transformers, have seen problems with efficiency such as cost, percentage of achieved remediation, and the possibility of producing toxic by-products.

The search for an efficient technique that could be applied on a large scale led to 'tribolysis' in 2019. Under TriboREMEDY, a European Union Horizon 2020 project, tribodevice, a newly designed system, aims to prove the concept of tribolysis for PCB degradation and cell disintegration of pathogens. The tribolysis process involves the dynamic mechanical rubbing process for initiating degradation in a tribodevice and the static immersion to complete the degradation.

This project aims to evaluate the efficiency of the tribolysis process in the degradation of PCBs, optimize the tribolysis process and translate conditions from SRV to tribodevice.

The objectives of this work are:
- Apply the tribolysis technology for PCBs, using 3,4-Dichlorotoluene
- Evaluate the rate consumption of 3,4-Dichlorotoluene
- Determine the minimum required time duration for initiating the degradation reaction based on the previously achieved 30 minutes duration.
- Determine the minimum required time duration for static immersion to achieve the maximum rate of DCT consumption
- Present the optimum parameters for the tribological process to the triboREMEDY consortium for the project continuance.

Methodology

In this chapter, the whole experimental procedures for this project are described. This includes developing the chemical compound for the experiment, the Reciprocating Sliding Friction and Wear Test (SRV), and the characterisation techniques employed in this study.

3.1 Materials

There are two main material groups for this experiment, which are necessary for the tribological process. The first group is the test fluid with the compound that needs to be degraded, which in this case was 3, 4-Dichlorotoluene (DCT), a less threatening substitute for PCB. The second group includes the surfaces in contact, where one material is magnesium alloy AZ91A and the other an ASTM 52100 100Cr6 steel disc. The reciprocating motion in the SRV experiments was intended to create conditions to decompose the DCT in the test fluid. The friction energy in the system initiates the reaction and the as the oxide surface of the mg alloy wears off, the nascent surface of magnesium is exposed to the test fluid to assist the degradation reaction.

3.1.1 PCB Substitution: 3, 4-Dichlorotoluene

Due to the high toxicity of PCBs and their classification as 'priority hazardous substances' in the EU, the experiments in this project could not be conducted with PCBs. Handling PCBs outside a critically controlled environment is not advised as inhalation may lead to cancer, fertility issues, and even death. Thus, for this experiment, PCB was substituted with a less threatening chemical compound, 3, 4-Dichlorotoluene (DCT).
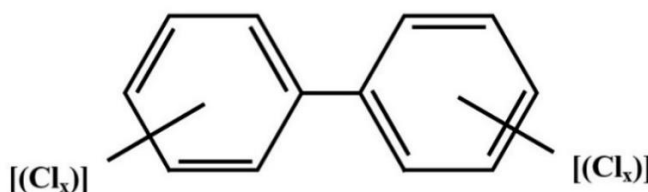
Figure 4: Chemical Structure of PCBs

PCBs are represented as $C_{12}H_{10-x}Cl_x$ with varying numbers and positions of the chlorine atoms (congeners) sharing the biphenyl structure, as seen in Figure 2.1. Like tetrachlorobenzyltoluenes (TCBTs), DCTs share similar polarities and

comparable volatilities with PCBs as well as a similar biodegradation process. The biodegradation of xenobiotic compounds like both PCBs and DCTs has been demonstrated through dehalobacter species with proven versatility in dehalogenation. The processes involve deoxygenation to form metabolites hydroxylated and subsequently, final degradation by meta ring cleavage to produce chlorinated benzoic acids . Based on these, DCT has been used as a substitute for transformer oil containing PCB. For convenience in the experimental handling and analysis, a concentration of 8wt% DCT dissolved in hexadecane was chosen for the experiments.

The following details of the compounds used are taken from the manufacturer's technical datasheets [97], [98].

- 3,4-Dichlorotoluene (DCT), $C_7H_6Cl_2$
- Hexadecane $C_{16}H_{34}$
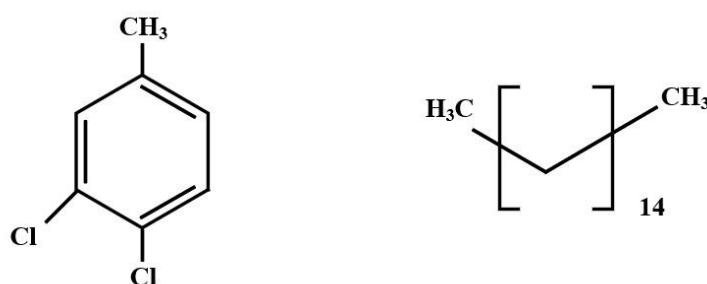
Figure 5: (a) Chemical Structure of 3,4-DCT and (b) Hexadecane

Each experiment uses 100 mg test fluid taking a 1% error allowance for the measurements [3,4-DCT (8mg) and $C_{16}H_{34}$ (92mg)]. The measured constituents in the fluid sample are listed below;

$$\boldsymbol{DCT}\ [C_7H_6Cl_2] \quad + \quad \boldsymbol{Hexadecane}\ [C_{16}H_{34}] \qquad \textit{Equation 4}$$
$$\boldsymbol{0.294g} \qquad\qquad\qquad \boldsymbol{3.43g}$$
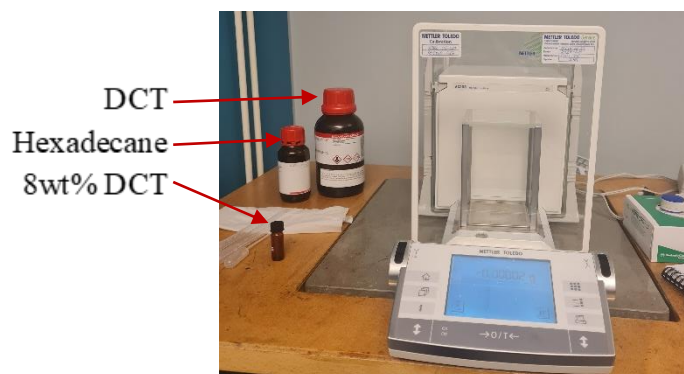
Figure 6: The sample development is shown alongside the Mettler Toledo Analytical Balance for sample measurement

3.1.2 Disc and Cylinder for SRV Setup

The upper and lower specimens in the SRV tribometer setup include a cylinder and disc respectively. There are three SRV experimental set-ups in this project and the variations involve the MG alloy surface finish and interchanging the material type in the upper and lower specimen.

The following are the details of the materials

- *ASTM 52100 Bearing Steel:* This is the standard disc used as a lower specimen in SRV [99]. It is the material for the lower specimen disc in the first two set-ups and the upper specimen cylinder in the third set-up.
- *AZ91A Magnesium Alloy:* This is the second material in the interface, and it is the most important for the degradation reaction. The samples are produced in cylinder and disc shapes from a sintered magnesium alloy bar. In this project, magnesium was chosen for its rapid reaction with chlorine to form metal chlorides. Magnesium is readily recycled and easily machined which are optimum properties required in this experiment . The contact surface of the samples was machined in two forms; *electrical discharge machining (EDM)* and *lathe machining*. The dual machining processes were applied to discover the surface type that improves the reaction in the experiment. While lathe machining creates a finer surface, EDM-machined surfaces tend to have high surface roughness. Degradation initiation in this experiment is highly dependent on the reaction at the interface. Therefore, the sample machining and manufacturing process were carefully considered. The sintered magnesium alloy was selected for its porosity as the powder metallurgy process of sintering creates cracks and pores between particles during the compaction [102]–[104].

The table below describes the three set-ups applied in the SRV;

Table 1: SRV Experimental Set-Ups

Set-Up	Upper Specimen	Lower Specimen
1.	EDM Mg Cylinder	Steel Disc
2.	Lathe Mg Cylinder	Steel Disc
3.	Steel Cylinder	Mg Disc

While the lower sample remains constant in the first and second set-ups, the differently machined cylinder samples presented a case to analyse the influence of the machining type. The third set-up presents an inverse of the first set-up for comparison against it.

(i)

(ii)

(a) Upper Specimens   (b) Lower Specimens
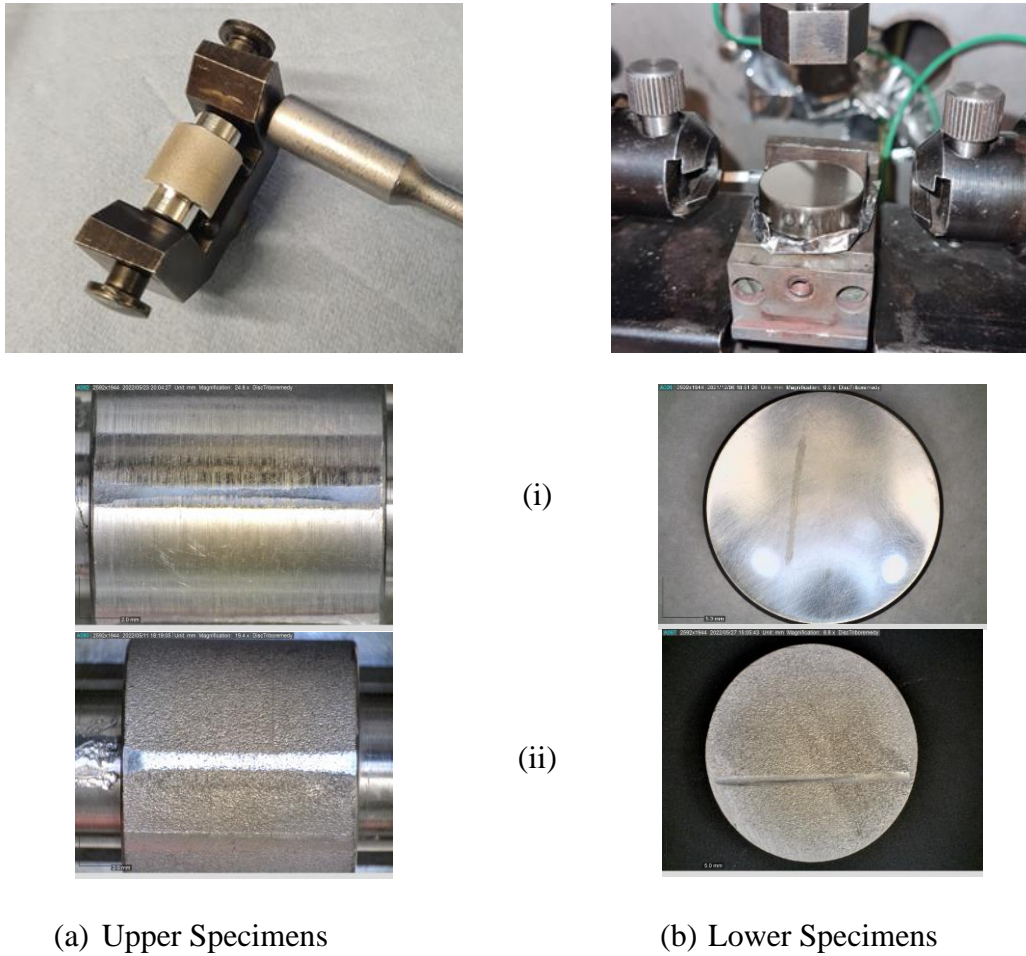
Figure 7: The SRV setup including sample holders for the upper and lower specimens. The upper specimen (a) sintered magnesium alloy shows the contact area processed with (i) electrical discharge machining and (ii) lathe machining. The lower specimen, (b)i. the standard ASTM 52100 steel disc is placed in an improvised sample collector (a foil), to check for and to collect any sample leakages from the experiment. The magnesium alloy disc is shown in (ii), made according to the dimensions of the steel disc.

3.2 The Reciprocating Sliding Friction and Wear Test (SRV)

The tribolysis process is replicated using the SRV in Figure 2.3 in a cylinder-on-disc model for a line contact. The reciprocating sliding movement of the cylinder on the disc causes friction and wear on the surfaces. As the less hard material, the magnesium cylinder experiences more significant wear, therefore, exposing a nascent surface of magnesium that reacts with the 8wt% DCT.
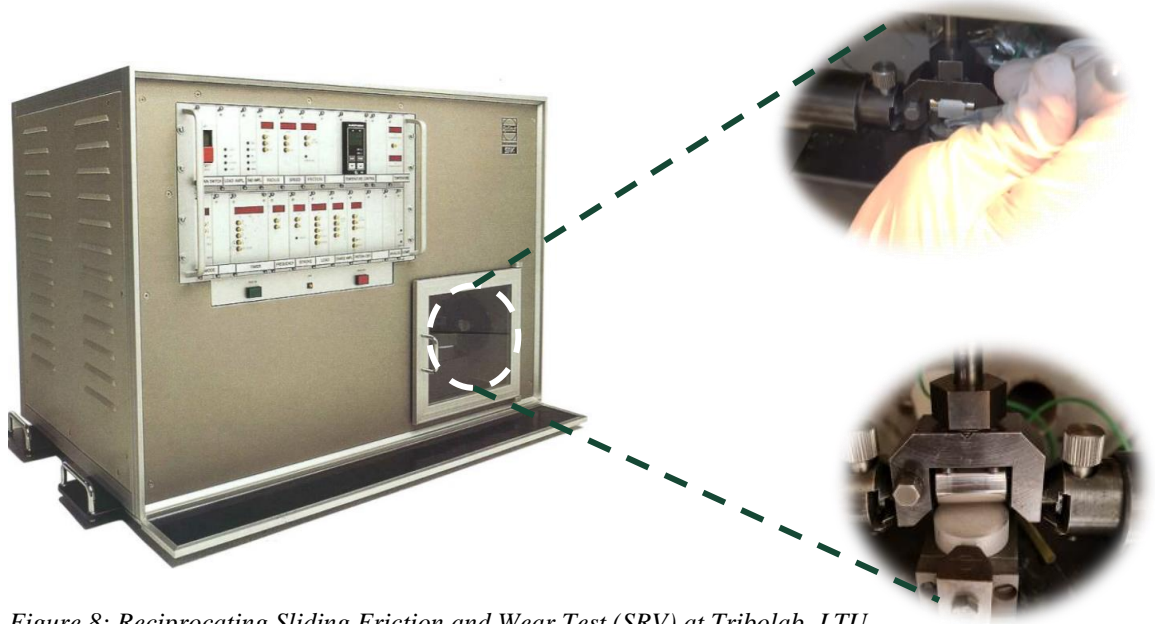
Figure 8: Reciprocating Sliding Friction and Wear Test (SRV) at Tribolab, LTU

Each sample set was placed in the SRV machine following a calibration procedure to ensure that results were consistent throughout the experiments. The applied parameters for all the experiments are presented in Table 1.

Table 2: Parameter for SRV Setup

PARAMETERS	VALUES
LOAD	15 N
ATMOSPHERE	Nitrogen
FREQUENCY	50 Hz
TEMPERATURE	30 °C
STROKE LENGTH	2000 µm

In addition to the wear information, data from the SRV experimental setup were collated for further investigation, such as variations in the coefficient of friction used to compute energy consumption.

3.3 Characterization Tools

This section describes the characterization methods used for the test samples, including the cylinder, disc, and fluid samples.

3.3.1 Digital Optical Microscopy

To observe the surfaces of the cylinder sample, the Dino Capture Digital Microscope at Tribolab, LTU was used to examine:

- The dimensions of the wear scar for computing the wear volume
- The variations in the wear scare size (length and width)

For this report, little or no focus was placed on characterizing the ASTM 52100 disc as the wear information was negligible. The Mg AZ91A cylinder provided more helpful information on wear and material loss.
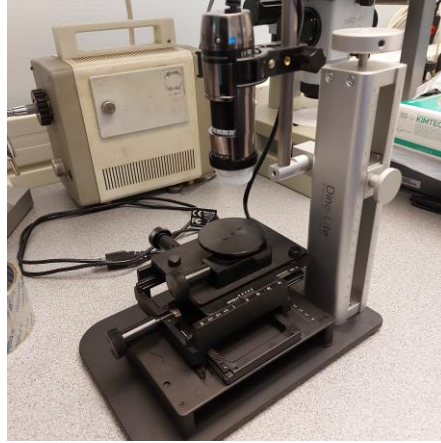
Figure 9:Dino Capture Digital Microscope at Tribolab, LTU

3.3.2 Fourier Transform Infrared Spectroscopy (FTIR)

FTIR is a renowned chemical analysis tool applied in this project to determine the success of the degradation process. Within the FTIR system is a spectral database containing several organic compounds. During the fluid analysis, the FTIR generates a spectrum that can provide information on the composition of the fluids [105], [106]. The FTIR analysis is described in subsequent sections below.

Figure 10: Fourier-transform infrared spectroscopy, showing a spectra on monitor screen [107]

3.3.3 Scanning Electron Microscope with Energy-Dispersive Spectroscopy (SEM-EDS)

Scanning electron microscopy (SEM) is one of the most popular analysis tools in the field of materials science. Combined with energy-dispersive spectroscopy, SEM-EDS allows for the measurement of important and desirable details such as the elemental composition in small selected sections of sample surfaces. It is also commonly referred to as SEM-EDX and can be applied by inputting the EDS/EDX tool in the SEM test chamber. In this project, SEM-EDS was applied to analyse the wear particles generated after the SRV experiment.

3.4 Chemical Analysis: Reference Fluids and FTIR Analysis

As mentioned above, FTIR was the main tool used for the chemical analysis of the test fluid in these experiments. The spectrum produced in the FTIR was analysed based on calibration or a basis of comparison to calculate degradation. The subsections below provide details about the spectra information, creating reference fluids, and creating a calibration for the FTIR analysis.

3.4.1 The Principle of the FTIR Spectroscopy

The FTIR is a development that is based on Infrared Spectroscopy but with an increase in the speed of the analysis. Infrared Spectroscopy is an aspect of spectroscopy that focuses on examining the infrared region of the electromagnetic spectrum. When infrared lights are directed at the sample, it incites an intra-band transition of electrons from one state within the same band. The intra-band transition cause vibrations which are analysed to provide information on the band structure. These details are specifically obtained within the mid-infrared region (4000–200 cm^{-1} wavenumbers) which covers the fundamental vibrations and the rotation-vibration structure of small molecules. The mid-infrared region can further be subdivided into two regions; fingerprint (in the 400–1400 cm^{-1} absorbance range) and functional group (between 1400–4000 cm^{-1}), still based on wave number. Thus, through Infrared Spectroscopy, functional groups and structural details of a compound can be identified [108].
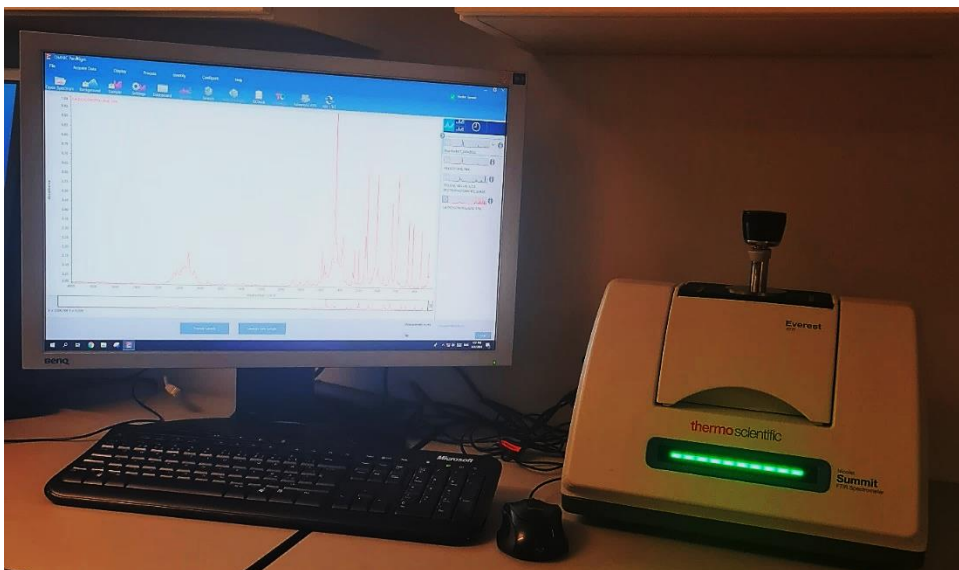
Figure 11: FTIR Equipment at Tribolab

In this project, the absorbance spectra were obtained using the more versatile **Attenuated Total Reflectance (ATR)** sampling technique. The ATR-FTIR system was the better sample technique due to the reasons below;

    a. The samples that could be collected after the experiments were too minute to be applicable in the transmission tube as seen in Figure 24.

    b. No sample preparation is required because of the precision with ATR-FTIR

    c. ATR is very applicable for liquid samples and in this case of an open sample holder, there was no fear of evaporation of the fluid sample.

Furthermore, ATR uses the medium of high refractive index crystals called ATR-crystals to ensure sufficient absorbance of the infrared rays. The basic details of the FTIR device used are in Table 3 as follows;

Table 3: Specifications of the FTIR Device

Smart Accessory Title	Everest ATR
Model	Nicolet Summit
Crystal Type	Diamond
Beam splitter	KBr
Detector	DTGS KBr

3.4.2 Absorbance and Peaks

Recalling section 2.1.1 above, the primary test fluid used in this project was 8wt% DCT produced from 99% Hexadecane and 97% 3,4 DCT. Thus, the spectra of both hexadecane and DCT were obtained from the FTIR and compared. The comparison showed relativities and differences in peaks, giving an idea of the

important regions as seen in Figure 10. In addition, comparing the spectra of Toluene to DCT was useful in confirming the peaks that represented the chlorination bonds. This is important because DCT is a chlorinated form of toluene. 3,4-DCT is an isomer of DCT which is produced in small amounts during the direct chlorination process of Toluene. The process also produces high amounts of 2,4 and 2,5-DCT isomers along with low amounts of 2,3- and 2,6-DCT [109], [110].

The objective of the experiments was dehalogenation, breaking the C–Cl aromatic bonds which are within the mid-infrared region. The C–Cl vibration stretches usually appear in the fingerprint region, between 850 – 550 cm^{-1}. However, the peak variations in the higher wave number range also contain very useful information about the nature of the bonds between carbon and hydrogen and carbon and oxygen. For example, the noticeable sharp peaks between regions between 2500 – 3100 cm^{-1} are characteristic of the C–H stretches [105], and this is observed especially in the spectra of hexadecane (alkane stretches) and toluene (alkene stretches) in Figure 10 and 11. Other recognizable peaks are within 1465 – 1365 cm^{-1}, 1150 – 1050 cm^{-1}, and 1050 – 1040 cm^{-1}. The absorption bands between 1100 – 1000 cm^{-1} are indicative of bonds including C-H deformation or C-O and C-C stretches. 1465 – 1365 cm^{-1} absorption bands also indicate C–H bends [105], [106].
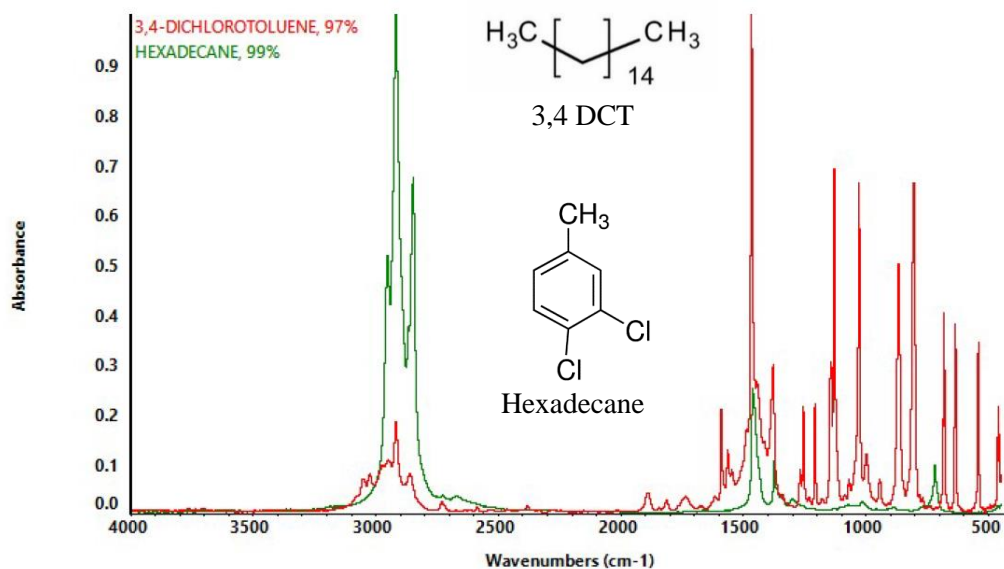

Figure 12: FTIR Spectra of 3,4-DCT and Hexadecane
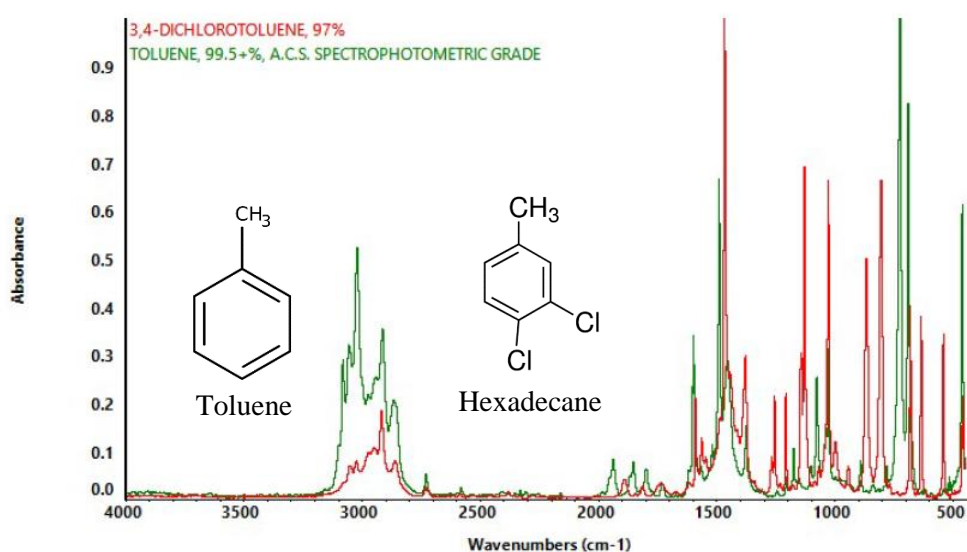
Figure 13: FTIR Spectra of 3,4-DCT and Toluene

3.4.3 Reference Fluids and Calibration

To create the calibration for the FTIR analysis, four reference fluids were created. The fluids were measured following weight calculations in section 2.1.1 containing varying proportions of DCT as follows;

    a. 8wt% DCT

    b. 4wt% DCT

    c. 2.4wt% DCT

    d. 0.8wt% DCT

For the purpose of this project, 'reference fluids' simply laid a basis for calibrating the measurement. Each reference fluid was measured in triplicate series using the FTIR device in order to justify the spectra results. Prior to these tests, the FTIR accuracy was also evaluated by measuring fluid samples (with known spectra) such as hexadecane and heptane and comparing them to the spectra in the database.

The spectra of 97% 3,4 DCT and 99% Hexadecane were compared to the reference fluids in Figure 12. A MATLAB script was applied to process and analyse the data in the FTIR spectra. In the script, the spectra were processed to obtain a similar baseline for comparison. This was obtained by subtracting the background data from the below plot curves. The script provides data on the percentage of DCT in the reference fluids. In this case, hexadecane can be likened to the background fluid and the DCT the additional compound. The level of DCT in the reference fluids is determined in wt% through routines in the MATLAB script. In Figure 12 below, the data points of thirteen major peaks are highlighted out of all the peaks. It is important to note that all the peaks fall within the wave number ranges already described above. In the MATLAB script, the thirteen data

points (major peaks) are represented in thirteen columns while the rows are representative of each fluid. Hence, there are six rows with the data of the four reference fluids, DCT, and hexadecane.

The spectra in Figure 12 show varying peaks in all the fluids. It is important to note that almost all fluids peaked within the same wave number, howbeit with different levels of absorbance. However, in some wave numbers highlighted, either DCT or hexadecane have no peaks or absorbance. For example, at 720 cm^{-1}, the DCT spectra showed no absorbance peak, giving indications that the peaks there are only categorical to hexadecane. For all the fluids with hexadecane, the peak at 720 cm^{-1} was at the same absorbance level as shown in the zoomed image in Figure 13. Whereas, from 808 cm^{-1} – 1146 cm^{-1}, all fluid spectra showed negligible levels of absorbance except DCT. Therefore, the peaks here are categorical to significant DCT content, and not fluids highly diluted with hexadecane.
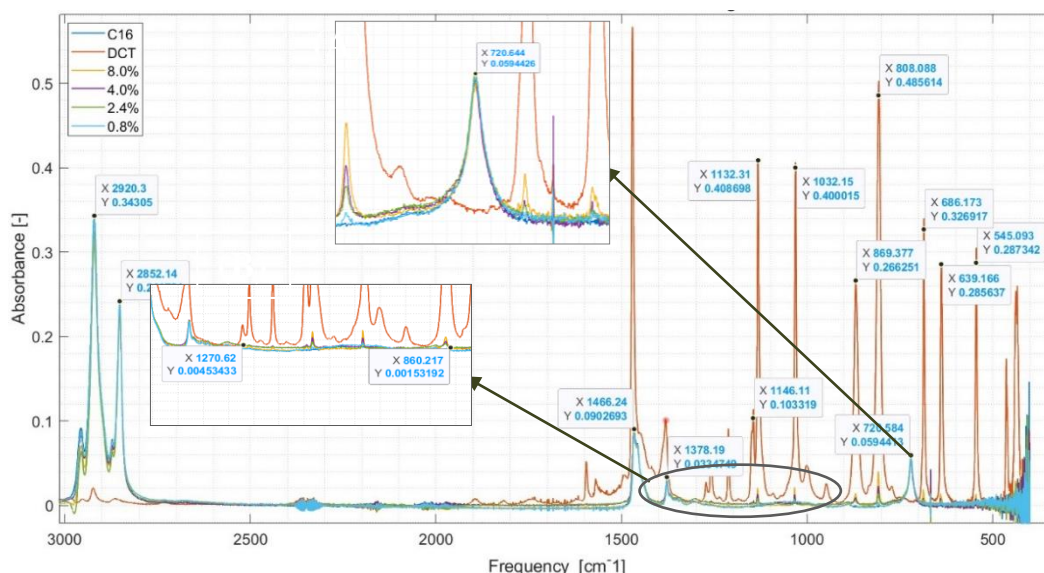
Figure 14: FTIR Spectra of DCT, hexadecane, and four reference fluids. (A) shows a peak of 720 cm^{-1} absorbance appearing in all fluids except DCT while (B) shows a range where only the DCT spectra showed any absorbance/peaks.

These points of exclusivity between DCT and hexadecane marked the basis for creating the calibration from the script. The peaks categorical to DCT are referred to as DCT-peaks while those categorical to hexadecane are C$_{16}$-peaks. Thus, the percentage of DCT in the reference fluids is generated based on the absorbance levels of DCT-peaks relative to the absorbance levels of C$_{16}$-peaks *in each fluid spectra*.

The MATLAB routine is described simply in the equation below;

$$\frac{DCT peaks\ in\ Reference\ Fluids\ Spectra\ [relative\ to\ DCT]}{C_{16} peaks\ in\ Reference\ Fluids\ Spectra\ [relative\ to\ C_{16}]} =$$

Equation 5

$$= \frac{Reference\ Fluids\ Spectra\ [Only\ DCTpeaks])}{DCT\ Fluid\ Spectra\ [Only\ DCTpeaks])} \bigg/ \frac{Reference\ Fluids\ Spectra\ [Only\ C_{16}peaks]}{C_{16}\ Fluid\ Spectra\ [Only\ C_{16}peaks]}$$

Equation 6

Following the routine described above, the DCT wt% results from the MATLAB processing were plotted against the already known wt% of the reference fluids. The calibration in Figure 13 showed a linear relationship that confirms the validity of the data process. Hence, the test fluids in this project were analysed using the same script. The results are discussed in the subsequent sessions.
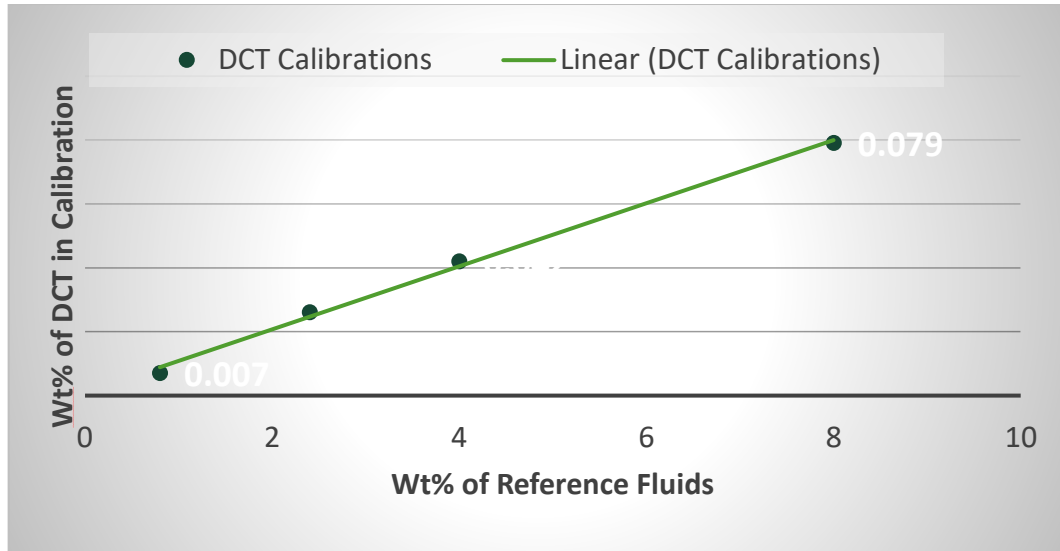
Figure 15:Calibration of Reference Fluid for Analysing Test Results

3.5 Experimental Design

In the previous phase of the project, the tribolysis experiments performed on the SRV provided the following information:

- ~80% of the DCT was consumed after a 30 minutes SRV experiment (rubbing) in a Nitrogen atmosphere [$\mu_{avg} = 0.26$]
- A 30 minutes SRV experiment (rubbing) in Nitrogen followed by 22-hour static immersion resulted in 100% consumption of the DCT.

The present research questions are culled from the objectives of this research.

1. What is the minimum required dynamic (rubbing) time duration for initiating the reaction?
2. What is the rate of consumption during the static immersion?
3. Which experimental setup can provide the most optimum results?

The test matrix in Table 2 was developed for the research to advance the results from experiments in the previous phase of the project.

Table 4: Test Matrix – Time Duration in Dynamic or Static Conditions

S/N	Dynamic Rubbing	Static Immersion	Intended Evaluation
1.	30 minutes		*Time required to initiate the reaction after timed dynamic rubbing*
	15 minutes	0	
	5 minutes		
2.	5 minutes	25 minutes	*Time required to initiate reaction within 30 minutes total duration*
	15 minutes	15 minutes	
	30 minutes	0	
3.	15 minutes	0	*DCT consumption during static immersion following 15 minutes of dynamic rubbing*
	15 minutes	15 minutes	
	15 minutes	2 hours	
	15 minutes	6 hours	
	15 minutes	24 hours	
4.	30 minutes	0	*The three set-ups described in section 3.1.2*

Results and Discussions

This chapter presents the results from the experiments carried out in the course of this thesis project. The report includes the tribological characterization for wear and friction analysis while more emphasis is placed on the chemical analysis.

4.1 Friction

The tribological characterization was taken from the tribometer test experiment on the SRV, and the results obtained for the Coefficient of Friction are presented in Figure 14, Figure 15, and Figure 16. The values described in the figures neglected the run-in phase, accounting only for the steady-state values of the coefficient of friction.

To begin the experiments, a trial test in Air was conducted to be compared with the experiments from the previous project phase. The coefficient of friction values was in the range of $\mu = 0.65\text{-}0.75$ and was unsteady and fluctuating even after the run-in stage. It aligned with the values from the previous phase of the project where $\mu_{avg} = 0.69$. With this comparison in check, the tests in Nitrogen were conducted.

In the Nitrogen atmosphere, more steady and lower values were observed. After the run-in phase, the friction values in all the tests were steady and within a variation range of $\mu = 0.288\text{-}0.416$, which is similar to the values obtained in the experiments of the previous project phase, $\mu_{avg} = 0.26$. The previous test for the comparison was also conducted in a nitrogen atmosphere.

Comparing the results above confirmed that the Nitrogen atmosphere gives more steady friction values and lower friction values. The sections below offer more details about the friction results.

4.1.1 Friction: Comparing Tests at Constant Duration of Dynamic Rubbing (30 minutes)

Conducting the experiments in a nitrogen atmosphere proved the steadiness of the coefficient of friction. Therefore, the next SRV experiments with a thirty minutes duration helped to evaluate the consistency of the experimental results.

In Figure 14, the coefficient of friction from the five series of SRV experiments is described in a chart. The values were within a close range ± 0.05 as $\mu_{avg} = 0.297 - 0.395$.
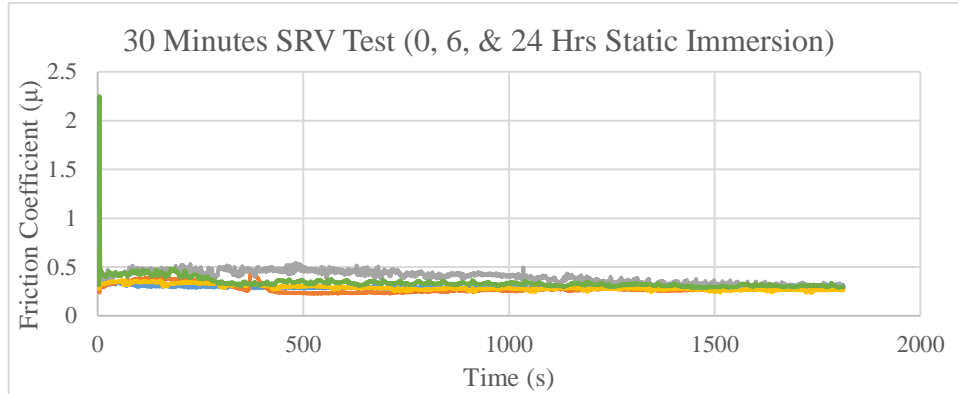
Figure 16: Results from Five SRV Experiments at Constant Duration of Dynamic Rubbing

4.1.2 Friction: Varying Duration of Dynamic Rubbing

Figures 15 and 16 show the coefficient of friction values when the SRV experiments were varied from five to thirty minutes according to the test matrix in the previous section. Irrespective of the variation, the coefficient of friction values still fell within a close range except for a single case (5 Mins, Run 1) where the value increased progressively until the end of the experiment. This outlier could be connected to errors in the sample production or SRV setup which would be better addressed in subsequent sections.
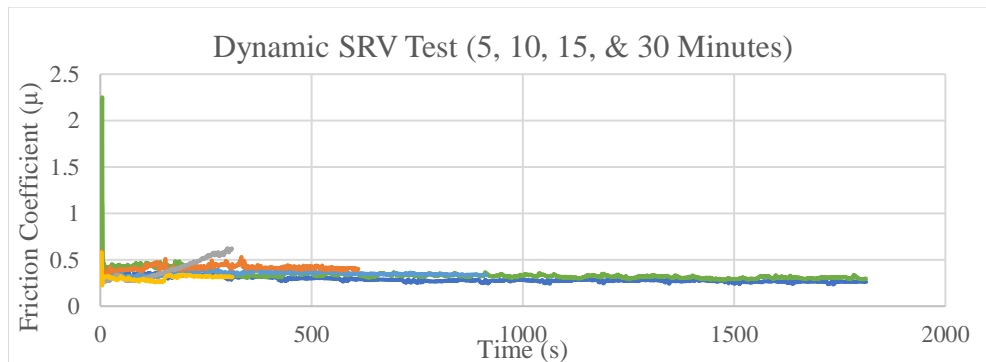
Figure 17: Results from SRV Experiments with Varying Duration of Dynamic Rubbing
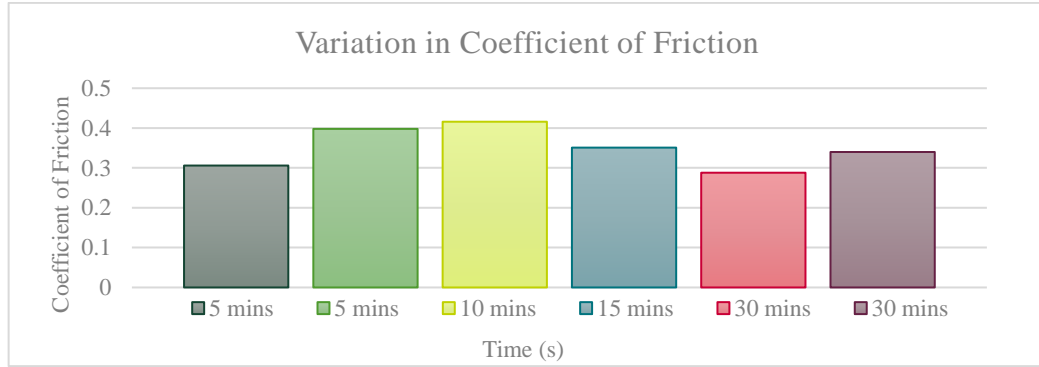
Figure 18: Results from SRV Experiments showing the variation in coefficient of friction for varying duration of dynamic rubbing

4.1.3 Friction: Comparing Three Experimental Set-Ups

The SRV experiments for the second set-up presented the lowest friction values compared to the other two, as seen in Figure 17. The three experiments had the same duration (30 minutes) and the same atmosphere (nitrogen). In subsequent sections, these values would be related to the wear volume and degradation levels.

	SU_1	SU_2	SU_3
Friction Coefficient, μavg	0.2975	0.2105	0.7555
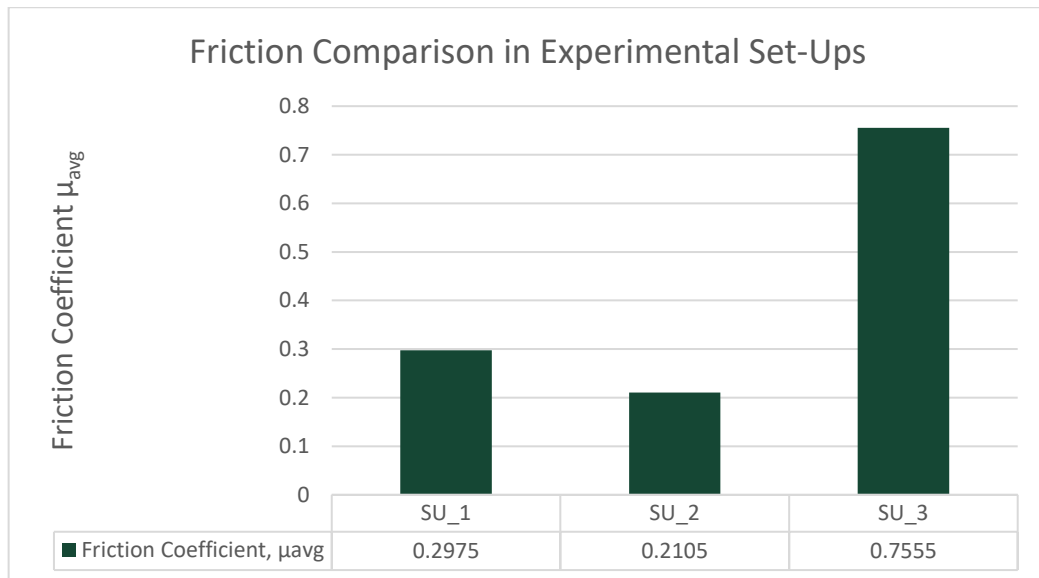
Figure 19: Comparing Friction Results from Three SRV Experiments of 30-Minutes Duration

4.2 Wear

For evaluating the wear, the focus was placed on the magnesium alloy samples. The ASTM 52100 steel discs and cylinder were not considered as the wear tracks provided negligible information. The cylinder samples were analysed using optical microscopy to view the wear information. The wear scars seemed quite
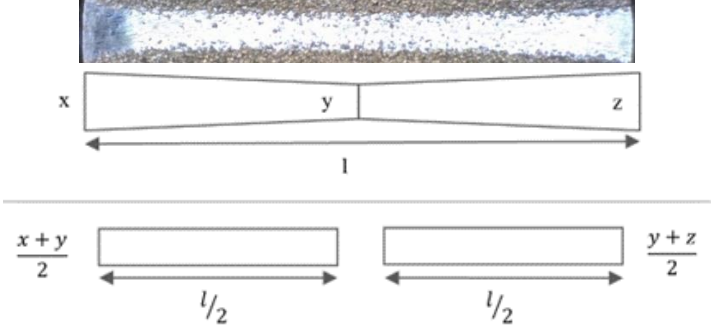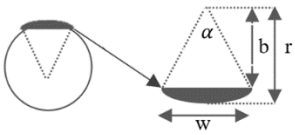
consistent within tests of the same parameters. Careful steps were taken to maintain the sample handling, setup, and arrangement throughout the series of experiments.

Following the optical microscopy characterization, the images of the wear scars on the magnesium samples are presented in Table 5 and the wear volume and mass are in Figures 18 and 19.

4.2.1 Variation of Wear and Magnesium (Mg) Mass Loss

The wear scars in these experiments were small-scale with very negligible depths. As shown in Table 5 and Figure 19, the wear scars on the samples have very minimal values in depth compared to the length and width. Therefore, certain approximations were necessary to calculate the wear volume and magnesium mass loss due to wear. The equations are described in Table 5 below;

Table 5: Description of Equations and Calculations Used for Magnesium Mass Loss Calculations

Area, $A =$	$= \left(^l/_2\right)\dfrac{x+y}{2} + \left(^l/_2\right)\dfrac{y+z}{2} \quad = \quad l\dfrac{(x+2y+z)}{4}$ $= lw$ Width, $[w = \dfrac{(x+2y+z)}{4}]$
	Cylinder radius, $r = 7.5mm$ Sector Angle, $\alpha = 2 * \arcsin\left(^w/_{2r}\right)$ Sector Length, $s = \alpha * r$ Wear Depth, $h = r * \left(1 - \cos\left(^\alpha/_2\right)\right)$ Distance of wear depth from centre, $b = r - h$
Cross-Sectional Area, $C.A =$	$= ^1/_2 \left((r * s) - (b * w)\right)$
Wear Volume of Mg, V_{mg}	$= l * C.A$
Wear Mass of Mg, $M_{mg} =$	$= V * \rho$ Density of MgAZ91A, $\rho = 1.82 \ g/cm^3$

The wear scars had a hyperbolic shape that was approximated to two isosceles trapezoids joined at one of the parallel sides. The accurate dimensions of the wear scar, x, y, z and l were obtained using the Dino Capture Digital Microscope and used for the calculations. However, the graphical representations of the wear scar are just an approximation and not following the exact dimensions.

Each test was conducted four times to confirm the consistency of the results. In Figure 18 below, the amount of worn magnesium (Mg) was compared for only the first set-up. In this setup, the magnesium alloy cylinder experienced wear which increased progressively with an increase in the duration of the SRV experiment (from five to thirty minutes). This data would be further analysed in Section 3.3, revealing the correlation to the degradation levels of DCTs in the test fluid.
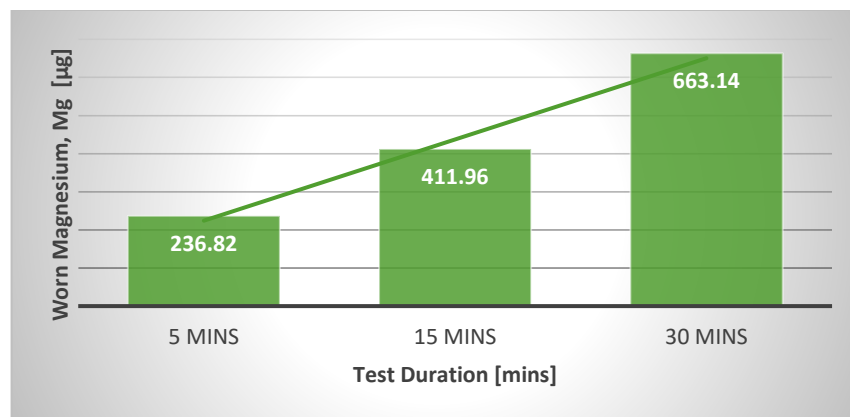
Figure 20: Worn Magnesium in Varying SRV Experiment Duration

4.2.2 Set-Up Variations: Wear and Magnesium (Mg) Mass Loss

The magnesium loss due to wear was analysed in Figure 19 for each experimental set-up. The first set-up produced the most wear on the magnesium sample which was about seventeen (17) times the third set-up and five (5) times the second set-up. The width of wear scars in the selected samples can be compared to validate the mass loss values. In this case, the x-parameter in the first sample is almost four (4) times the second set-up. The amount of mass loss due to wear will be further assessed in relation to the percentage of degraded DCT.
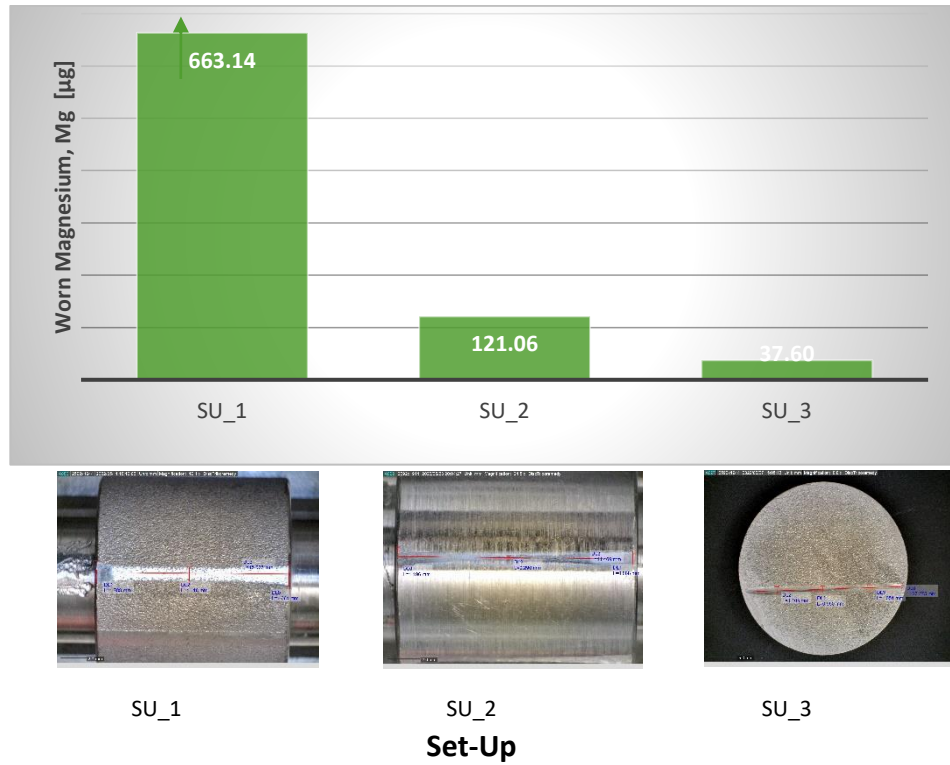
Figure 21: Magnesium (Mg) Loss on three sample set-ups

4.3 Chemical Composition-Degradation

In this project, degradation is observed in the breaking of the C–Cl aromatic bonds in the test fluids. In section 2.4, the reference fluids, FTIR spectra, and MATLAB analysis for the dehalogenation process have been explained in detail. Hence, all the results have been obtained following the script that produced the calibration in Figure 12. It is important to note that static immersion was not relevant in the wear and friction analysis. In this section, the influence of static immersion in the nitrogen atmosphere would be examined.

4.3.1 DCT Degradation: Varying SRV Experiment Duration

In the first set of experiments, the parameters maintained are as follows;
  a. First set-up: Mg alloy cylinder on steel disc sample.
  b. Dynamic Duration: 5, 15, and 30 minutes
  c. Static Immerssion: 0 hr. The samples were removed and tested immediately after the SRV experiment ended.

The bar charts in Figure 20(i) give a visual representation of the level of differences in the degradation levels after each SRV experiment. From this, it is evident that only five minutes of rubbing in the SRV was sufficient to initiate the degradation reaction. Also, it can be observed that the duration of rubbing in the

SRV strongly influences the amount of DCT being degraded. The bar chart can be related to the mass loss in Figure 18 (also in the Figure 19 pop-up) which showed a corresponding increase in mass loss with an increase in SRV experiment duration. Hence, the continuous creation of a nascent surface due to wear leads to a higher rate of reaction between DCT and Mg in the nitrogen environment. Through Figure 20(ii), the trendline can be seen showing a linear proportional relationship between the duration of the experiment and the amount of DCT being degraded. The rate of degradation is between 2-3% per minute.
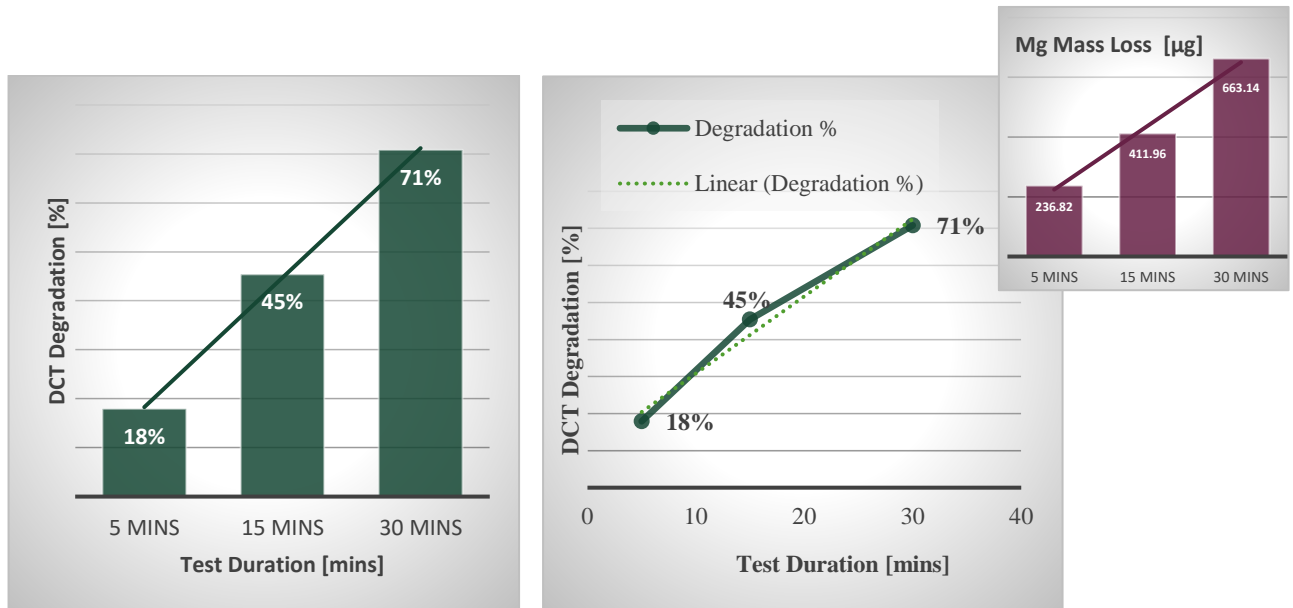
Figure 22: Variation of DCT Degradation with Time; 20(i) shows a bar chart while 20(ii) gives a more representative chart and trendline.

4.3.2 DCT Degradation: Evaluating Static Immersion Effect

The static immersion describes the period between the SRV experiment conclusion and the removal of the sample from the SRV chamber. In previous sections, the experiments did not include static immersion as the sample was removed from the chamber and tested immediately. In those cases, the test sample did not remain in a nitrogen atmosphere after the SRV experiment ended.

It was noted in the previous section that only five minutes of rubbing in the SRV could initiate degradation. The next questions were as follows;

1. After 5 minutes, is more rubbing more important for degradation or is it enough for the sample to be in the nitrogen atmosphere (without rubbing)?
2. What is the rate of degradation during static immersion?

To answer these questions, new experiments were performed with a focus on the effects of long and short static immersion.

Static Immersion: 30 Minutes Overall Test Time

This test series answered the first question in 3.3.2 by comparing the five (5) and fifteen (15) minutes SRV-dynamic tests to the thirty (30) minutes SRV-dynamic test. In this case, the 5 and 15 test series spent an additional 25 and 15 minutes respectively in the SRV test chamber in a nitrogen atmosphere. This brings the total test time to thirty minutes, including the dynamic and static sections.

15 minutes SRV test + **15** minutes static immersion

5 minutes SRV test + **25** minutes static immersion

From these test series, it's evident that further rubbing in the SRV for just 15 or 25 minutes has a significant effect on the degradation than static immersion. Compared to the full 30 minutes rubbing, the 15- and 5-minute run yielded very minimal improvement in degradation despite static immersion.
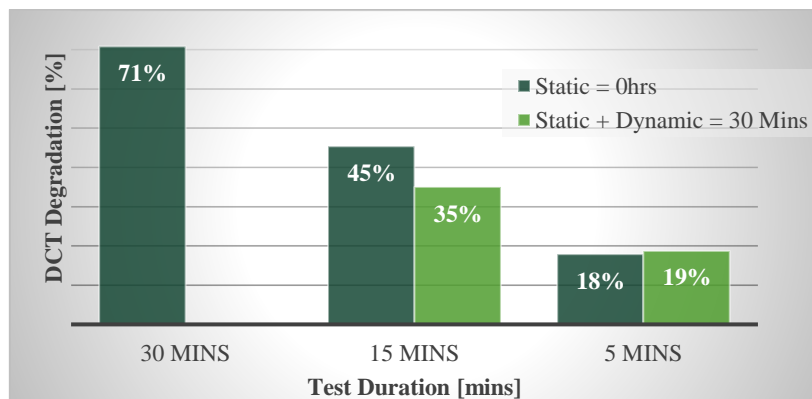
Figure 23: DCT Degradation with Short Static Immersion

As seen in Figure X above, the static time is too little to yield impactful differences. Therefore, short static immersions have little to no effects on the degradation even though the samples remain in the nitrogen atmosphere.

Long Static Immersions:

For the long durations of static immersions, the SRV experiment was fixed at fifteen (15) minutes. In the previous experiments, the 15 minutes rubbing/dynamic time yielded 45% DCT degradation. This was assumed to be sufficient degradation initiation, enough to measure the effect of further degradation during static immersions.
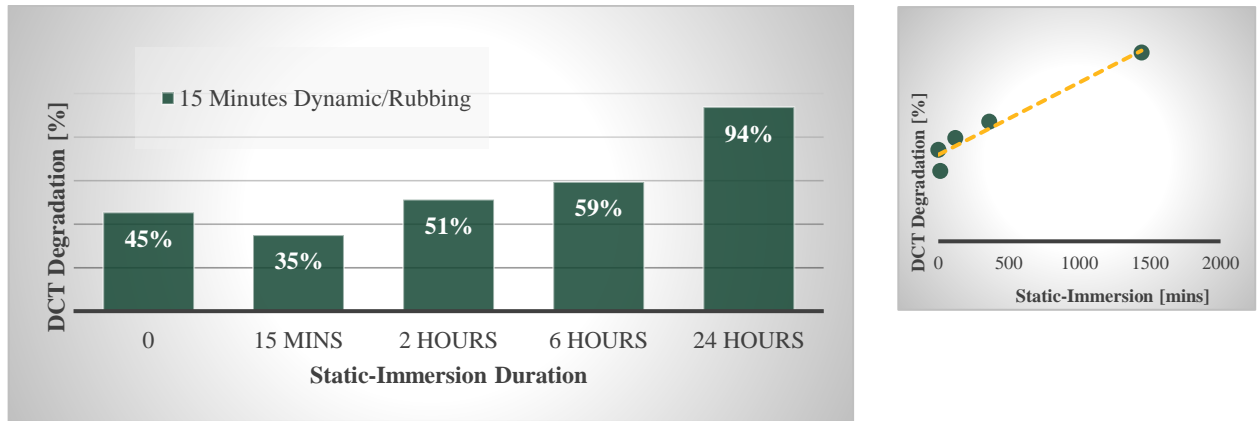
Figure 24: DCT Degradation with Long Static Immersion; 22(i) shows a bar chart while 22(ii) gives a more representative chart and trendline estimating 100% degradation at 27 hours.

According to Figure 22(i) above, the effects of static immersion can be observed as the DCT degradation increases progressively with time. Hence, after the initiation of the reaction from rubbing, the rate of degradation during immersion is ranged from 3.5% per hour in the beginning to about 2% per hour after the first six hours. A trendline (in Figure 22(ii)) can estimate a 100% degradation at 27 hours of static/wait time in the N_2 atmosphere.

4.3.3 DCT Degradation: Varying Experimental Set-Ups

The three set-ups were compared to determine the most optimum. The basis for comparison was primarily the level of DCT degradation and secondarily, the efficiency in relation to material loss.
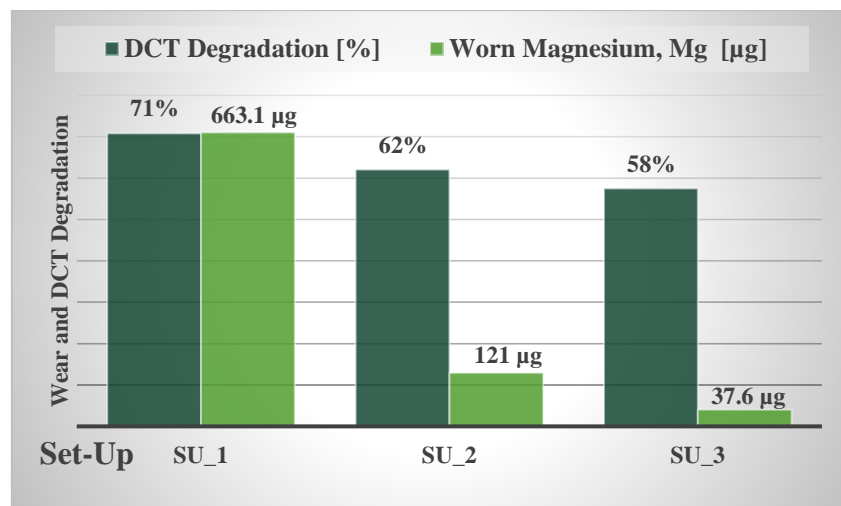
Figure 25: DCT Degradation in Multiple Experimental Set-Ups

Figure 23 above shows details of degradation levels in relation to mass loss from wear. The first noticeable result is in the close range of DCT degradation levels in all three set-ups. Although the third set-up has 95% less wear than the first, both

degradation levels remain in close range. This huge difference between the disc and cylinder magnesium alloy samples could be related to the overall surface area and the deformation type. Firstly, the cylinder samples present a higher overall contact area in the experiment. Secondly, the magnesium alloy is the lower specimen in the third set-up, unlike the first and second set-ups. In this case, the harder material, the steel cylinder sample, moves in a reciprocatory motion, penetrating through the disc in a ploughing effect as it plastically deforms instead of wearing off.

Furthermore, the mass loss disparity in set-up 1 and 2 show the implication of the sample finishing. In set-up-1, the higher wear volume is caused by the electrical discharge machining (EDM) which gave the Mg samples a rougher surface that promotes wear. Initially, the EDM was chosen with the idea that the rough surface would lead to wear and promote the creation of the nascent surface which would in turn promote the degradation reaction. However, from this test series, it is evident that the second set-up can achieve a close degradation level with 81% less material loss making it a more optimal option. Hence, the second set-up presents a promising lead with regard to material consumption in the economics of the process.

4.3.4 Particle Chemical Analysis from Scanning Electron Microscope with Energy-Dispersive Spectroscopy (SEM-EDS)

The chemical analysis of the wear particles was conducted following a procedure of (i) drying the test fluid on the steel disc using a vacuum drying device followed by (ii) the SEM-EDS analysis of the dried particles still on the steel disc.

Figure 26: Steel disc showing the fluid sample (i) immediately after the SRV experiment and (ii) after vacuum drying

The copper tape in Figure 24(ii) above helped to know the positioning and alignment of the steel disc while it's seated in the SEM chamber. The images in Figure 25 below show the steel disc and the fluid film on the surface. Through the

EDS tool, we can observe the presence of certain elements such as chlorine, magnesium, and steel. From both spectrums 1 and 2, and the estimated amount of these elements, the steel content is attributed to the steel disc as the rays penetrate past the film in spectrum 2.
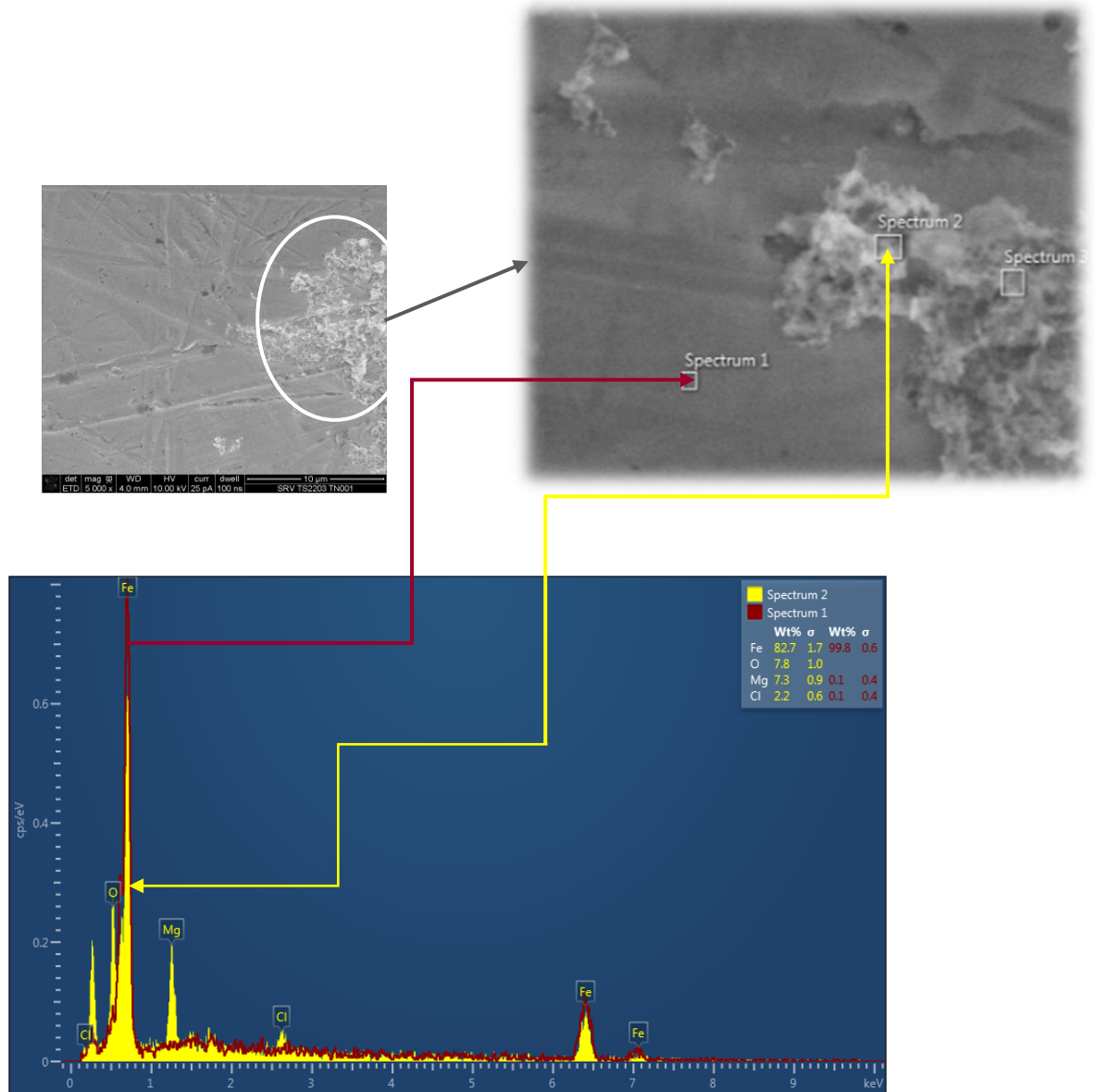

Figure 27: SEM-EDS Imaging showing the dried fluid film

Although this wear particle analysis did not give the exact form or compound in which the element appears, it indicated the presence of both magnesium (from the cylinder sample) and chlorine (from the test fluid). Hence, there's a confirmation of a fluid film bearing the elements from the two reacting surfaces.

Conclusion

This project is a continuance of the TriboREMEDY project and thus, aimed at improving the previously established parameters in the tribolysis process. In this investigation, the test matrix design entailed an initial repetition of the previously achieved test parameters before further test series and experiments towards a more optimum set of parameters. From the over fifty (50) sets of experiments conducted, the objectives and research questions have been answered as follows:

- The SRV tribology experiments from the previous project phase proven proved the tribolysis phenomena for degrading DCTs. In this current project, all the magnesium alloy samples experienced both wear and degradation. Irrespective of the shortness of the SRV test duration, each set-up showed that a reaction was initiated between the fluid sample and the exposed reactive magnesium nascent surface. The degradation was confirmed by FTIR tests. The chemical analysis using FTIR in this project gives more reliable information than the previous project phase based on the handling procedure. In this research, the sample fluids were tested immediately without alteration or dilution, unlike the past tests.

- Wear particles on the steel discs confirmed the presence of chlorine on the steel surface. Ordinarily, the DCT fluid samples evaporate after being left on a surface. The presence of chlorine and magnesium particles on the steel surface after vacuum drying proves that a reaction occurred. The reaction also led to the breaking of Carbon-Chlorine bonds and consequently, chlorine appearing in the dried film elemental analysis.

- The duration of the SRV test required to initiate the reaction has been confirmed to be five minutes or less. The rate of degradation is 2-3% per minute in the SRV (without static immersion). This implies that even a one-minute SRV experiment would initiate degradation as the nascent surface would have come in contact with the fluid. The values are an improvement from the previous experiment which hinged at 30-minute SRV experiments. Understanding the rate per time is useful towards creating the tribodevice in future.

- Static immersion effects are only observable in long durations. Hence, the influence of the nitrogen atmosphere on the experimental set-up (post-

SRV-test) is notable if the sample remains in the SRV chamber for long hours. This information has been confirmed with the 15-minutes SRV experiment and the analysis estimated a 100% DCT consumption at 27 hours of static immersion. However, previously, the 30-minute SRV experiment followed by a 22-hour static immersion achieved 100% DCT consumption. The difference between the 15- and 30- minutes SRV tests was a 5-hour difference in the static immersion to achieve 100% DCT consumption. While the rate of degradation during the SRV experiment is 2-3% per minute, the rate of degradation during static immersion is 3.5-2% per hour. Hence, it takes 22 hours for an initial 75% degradation to reach 100% and it takes 27 hours for an initial 45% degradation to reach 100%. Summarily, the rate of DCT degradation reduces with time in static immersion.

Within the same set-up, mass loss corresponded significantly to DCT degradation. However, between multiple set-ups, the change was neither proportional to the duration nor DCT degradation. This aspect is important for choosing the more effective setup in terms of material loss. Analysing this factor in relation to degradation level, the second set-up shows more efficiency with respect to mass loss.

Future Work

In this project, a thorough investigation has been done to understand the tribolysis process and provide more optimum parameters. Backing on the results and discovery made here, the following areas should be further explored in the next phase of the TriboREMEDY project:

- Minimizing energy consumption is important in producing an industrial-scale system. Hence, before designing the tribodevice a cost evaluation would be necessary to compare the 15- with the 30- minutes SRV tests with static immersion. While 50% of energy is conserved in the 15-min SRV process, an additional 5 hours in the nitrogen atmosphere is needed. This also implies energy consumption from power and gas. This economic and cost analysis would be imperative towards deciding whether to prioritize longer SRV duration or longer static immersions.

- With regards to efficiency in material consumption, further work should be put into the second set-up. From the results, the magnesium alloy cylinder with lathe machined surface finish yielded 81% less material loss than the cylinder with electrical discharge machining (EDM). Despite this huge disparity in material loss, the second set-up still produced 62% degradation, only 9% less than the first set-up. This goes to show that the second set-up may be a better case for the tribodevice. Exploring this with different durations of rubbing/SRV and static immersion may reveal more information for a better comparison of both set-ups.

- The wear particles and the dried film (post-experiment) should be studied in detail using more accurate tools which could give information on the nature and form of the chlorine compounds present.

Finally, static immersion still needs further studies. Based on the results obtained, static immersion has a much lower degradation rate (3.5-2% per hour) compared to degradation rates during SRV experiments (2-3% per minute). From the tests and analysis performed, it is still unclear whether the degradation in static immersion is due to the initiation reaction or due to the evaporation of the remnant DCT fluids after rubbing and initiation. This should be investigated in further studies.

References

[1] R. O. Anyasi and H. L. Atagana, "Biological remediation of polychlorinated biphenyls (PCB) in the environment by microorganisms and plants," *Afr. J. Biotechnol.*, vol. 10, no. 82, Art. no. 82, 2011, doi: 10.4314/ajb.v10i82.

[2] 张振国刘希涛 and X. L. Zhenguo ZHANG, "机械化学法降解氯代有机污染物的研究进展," 化工进展, vol. 40, no. 1, pp. 487–504, doi: 10.16085/j.issn.1000-6613.2020-0538.

[3] G. Cagnetta, J. Robertson, J. Huang, K. Zhang, and G. Yu, "Mechanochemical destruction of halogenated organic pollutants: A critical review," *J. Hazard. Mater.*, vol. 313, pp. 85–102, Aug. 2016, doi: 10.1016/j.jhazmat.2016.03.076.

[4] M. D. Erickson and R. G. Kaley, "Applications of polychlorinated biphenyls," *Environ. Sci. Pollut. Res.*, vol. 18, no. 2, pp. 135–151, Feb. 2011, doi: 10.1007/s11356-010-0392-1.

[5] M. M. Ododo and B. K. Wabalo, "Polychlorinated Biphenyls (PCBs) and Their Impacts on Human Health: A Review," *J. Environ. Pollut. Hum. Health*, vol. 7, no. 2, Art. no. 2, Oct. 2019, doi: 10.12691/jephh-7-2-3.

[6] N. B. Hopf, A. M. Ruder, and P. Succop, "Background levels of polychlorinated biphenyls in the U.S. population," *Sci. Total Environ.*, vol. 407, no. 24, pp. 6109–6119, Dec. 2009, doi: 10.1016/j.scitotenv.2009.08.035.

[7] O. US EPA, "Learn about Polychlorinated Biphenyls (PCBs)," Aug. 19, 2015. https://www.epa.gov/pcbs/learn-about-polychlorinated-biphenyls-pcbs (accessed Dec. 13, 2021).

[8] G. K. Robinson and M. J. Lenn, "The Bioremediation of Polychlorinated Biphenyls (PCBs): Problems and Perspectives," *Biotechnol. Genet. Eng. Rev.*, vol. 12, no. 1, pp. 139–188, Dec. 1994, doi: 10.1080/02648725.1994.10647911.

[9] "Aerobic Bio Degradation of Polychlorinated Biphenyls | PDF | Polychlorinated Biphenyl | Biodegradation," *Scribd*. https://www.scribd.com/document/61735291/Aerobic-Bio-Degradation-of-Polychlorinated-Biphenyls (accessed Oct. 10, 2022).

[10] O. Faroon and P. Ruiz, "Polychlorinated biphenyls: New evidence from the last decade," *Toxicol. Ind. Health*, vol. 32, no. 11, pp. 1825–1847, Nov. 2016, doi: 10.1177/0748233715587849.

[11] V. A. McFarland and J. U. Clarke, "Environmental occurrence, abundance, and potential toxicity of polychlorinated biphenyl congeners: considerations for a congener-specific analysis.," *Environ. Health Perspect.*, vol. 81, pp. 225–239, May 1989, doi: 10.1289/ehp.8981225.

[12] R. Jing, S. Fusi, and B. V. Kjellerup, "Remediation of Polychlorinated Biphenyls (PCBs) in Contaminated Soils and Sediment: State of Knowledge and Perspectives," *Front. Environ. Sci.*, vol. 6, p. 79, 2018, doi: 10.3389/fenvs.2018.00079.

[13] "EPA presentation to the Moffett Field Restoration Advisory Board on May 15, 2008, giving background on Poly-Chloronated Biphenyls (PCBs) - [PDF Document]." https://cupdf.com/document/epa-presentation-to-the-moffett-field-restoration-advisory-board-on-may-15-2008-giving-background-on-poly-chloronated-biphenyls-pcbs.html (accessed Jan. 19, 2022).

[14] B. Lindell and T. N. E. G. for C. D. of H. R. from Chemicals, *146. Polychlorinated biphenyls (PCBs)*. Arbets- och miljömedicin, Göteborgs universitet, 2012. Accessed: Oct. 10, 2022. [Online]. Available: https://gupea.ub.gu.se/handle/2077/28926

[15] "ATSDR - Toxicological Profile: Polychlorinated Biphenyls (PCBs)." http://medbox.iiab.me/modules/en-cdc/www.atsdr.cdc.gov//toxprofiles/tp.asp_id=142&tid=26 (accessed Dec. 13, 2021).

[16] J. N. Olson, O. Faroon, Syracuse Research Corporation, and United States, *Toxicological profile for polychlorinated biphenyls (PCBs)*. Atlanta, Ga.: U.S. Department of Health and Human Services, Public Health Service, Agency for Toxic Substances and Disease Registry, 2000. Accessed: Dec. 13, 2021. [Online]. Available: https://catalog.hathitrust.org/Record/003546659

[17] T. Ivanciuc, O. Ivanciuc, and D. J. Klein, "Modeling the bioconcentration factors and bioaccumulation factors of polychlorinated biphenyls with posetic quantitative super-structure/activity relationships (QSSAR)," *Mol. Divers.*, vol. 10, no. 2, pp. 133–145, May 2006, doi: 10.1007/s11030-005-9003-3.

[18] S. Tanabe, "PCB problems in the future: Foresight from current knowledge," *Environ. Pollut.*, vol. 50, no. 1, pp. 5–28, Jan. 1988, doi: 10.1016/0269-7491(88)90183-2.

[19] M. P. Jokinen, N. J. Walker, A. E. Brix, D. M. Sells, J. K. Haseman, and A. Nyska, "Increase in cardiovascular pathology in female sprague-dawley rats following chronic treatment with 2,3,7,8-tetrachlorodibenzo-p-dioxin and 3,3′,4,4′,5-pentachlorobiphenyl," *Cardiovasc. Toxicol.*, vol. 3, no. 4, p. 299, Dec. 2003, doi: 10.1385/CT:3:4:299.

[20] P. M. Lind, J. Örberg, U.-B. Edlund, L. Sjöblom, and L. Lind, "The dioxin-like pollutant PCB 126 (3,3′,4,4′,5-pentachlorobiphenyl) affects risk factors for cardiovascular disease in female rats," *Toxicol. Lett.*, vol. 150, no. 3, pp. 293–299, May 2004, doi: 10.1016/j.toxlet.2004.02.008.

[21] L. Rylander, A. Rignell-Hydbom, and L. Hagmar, "A cross-sectional study of the association between persistent organochlorine pollutants and diabetes," *Environ. Health*, vol. 4, no. 1, p. 28, Nov. 2005, doi: 10.1186/1476-069X-4-28.

[22] N. Codru, M. J. Schymura, S. Negoita, Akwesasne Task Force on Environment, R. Rej, and D. O. Carpenter, "Diabetes in relation to serum levels of polychlorinated biphenyls and chlorinated pesticides in adult Native Americans," *Environ. Health Perspect.*, vol. 115, no. 10, pp. 1442–1447, Oct. 2007, doi: 10.1289/ehp.10315.

[23] J. W. Chen, S. L. Wang, P. C. Liao, H. Y. Chen, Y. C. Ko, and C. C. Lee, "Relationship between insulin sensitivity and exposure to dioxins and polychlorinated biphenyls in pregnant women," *Environ. Res.*, vol. 107, no. 2, pp. 245–253, 2008, doi: 10.1016/j.envres.2008.01.004.

[24] "A Strong Dose-Response Relation Between Serum Concentrations of Persistent Organic Pollutants and Diabetes | Diabetes Care." https://care.diabetesjournals.org/content/29/7/1638 (accessed Dec. 13, 2021).

[25] D.-H. Lee, M. Steffes, and D. R. Jacobs, "Positive Associations of Serum Concentration of Polychlorinated Biphenyls or Organochlorine Pesticides with Self-Reported Arthritis, Especially Rheumatoid Type, in Women," *Environ. Health Perspect.*, vol. 115, no. 6, pp. 883–888, Jun. 2007, doi: 10.1289/ehp.9887.

[26] D.-H. Lee, I.-K. Lee, S.-H. Jin, M. Steffes, and D. R. Jacobs, "Association Between Serum Concentrations of Persistent Organic Pollutants and Insulin Resistance Among Nondiabetic Adults: Results from the National Health

and Nutrition Examination Survey 1999–2002," *Diabetes Care*, vol. 30, no. 3, pp. 622–628, Mar. 2007, doi: 10.2337/dc06-2190.

[27] C. Heilmann, P. Grandjean, P. Weihe, F. Nielsen, and E. Budtz-Jørgensen, "Reduced Antibody Responses to Vaccinations in Children Exposed to Polychlorinated Biphenyls," *PLOS Med.*, vol. 3, no. 8, p. e311, Aug. 2006, doi: 10.1371/journal.pmed.0030311.

[28] A. J. De Roos *et al.*, "Persistent organochlorine chemicals in plasma and risk of non-Hodgkin's lymphoma," *Cancer Res.*, vol. 65, no. 23, pp. 11214–11226, Dec. 2005, doi: 10.1158/0008-5472.CAN-05-1755.

[29] L. Hardell *et al.*, "Concentrations of polychlorinated biphenyls in blood and the risk for testicular cancer," *Int. J. Androl.*, vol. 27, no. 5, pp. 282–290, 2004, doi: 10.1111/j.1365-2605.2004.00489.x.

[30] L. Hardell *et al.*, "Adipose tissue concentrations of persistent organic pollutants and the risk of prostate cancer," *J. Occup. Environ. Med.*, vol. 48, no. 7, pp. 700–707, Jul. 2006, doi: 10.1097/01.jom.0000205989.46603.43.

[31] C. Zani, G. Toninelli, B. Filisetti, and F. Donato, "Polychlorinated Biphenyls and Cancer: An Epidemiological Assessment," *J. Environ. Sci. Health Part C*, vol. 31, no. 2, pp. 99–144, Jan. 2013, doi: 10.1080/10590501.2013.782174.

[32] N. M. Grindler, J. E. Allsworth, G. A. Macones, K. Kannan, K. A. Roehl, and A. R. Cooper, "Persistent Organic Pollutants and Early Menopause in U.S. Women," *PLOS ONE*, vol. 10, no. 1, p. e0116057, Jan. 2015, doi: 10.1371/journal.pone.0116057.

[33] G. M. Buck Louis *et al.*, "Persistent environmental pollutants and couple fecundity: the LIFE study," *Environ. Health Perspect.*, vol. 121, no. 2, pp. 231–236, Feb. 2013, doi: 10.1289/ehp.1205301.

[34] M. Denham *et al.*, "Relationship of Lead, Mercury, Mirex, Dichlorodiphenyldichloroethylene, Hexachlorobenzene, and Polychlorinated Biphenyls to Timing of Menarche Among Akwesasne Mohawk Girls," *Pediatrics*, vol. 115, no. 2, pp. e127–e134, Feb. 2005, doi: 10.1542/peds.2004-1161.

[35] B. Fimm *et al.*, "Neuropsychological effects of occupational exposure to polychlorinated biphenyls," *NeuroToxicology*, vol. 63, pp. 106–119, Dec. 2017, doi: 10.1016/j.neuro.2017.09.011.

[36] H. J. Strek and J. B. Weber, "Behaviour of polychlorinated biphenyls (PCBs) in soils and plants," *Environ. Pollut. Ser. Ecol. Biol.*, vol. 28, no. 4, pp. 291–312, Aug. 1982, doi: 10.1016/0143-1471(82)90146-5.

[37] A. C. Dietz and J. L. Schnoor, "Advances in phytoremediation.," *Environ. Health Perspect.*, vol. 109, no. suppl 1, pp. 163–168, Mar. 2001, doi: 10.1289/ehp.01109s1163.

[38] P. J. Harvey *et al.*, "Phytoremediation of polyaromatic hydrocarbons, anilines and phenols," *Environ. Sci. Pollut. Res.*, vol. 9, no. 1, pp. 29–47, Jan. 2002, doi: 10.1007/BF02987315.

[39] C. Tu *et al.*, "PCB removal, soil enzyme activities, and microbial community structures during the phytoremediation by alfalfa in field soils," *J. Soils Sediments*, vol. 11, no. 4, pp. 649–656, Jun. 2011, doi: 10.1007/s11368-011-0344-5.

[40] S. Dushenkov, Y. Kapulnik, M. Blaylock, B. Sorochisky, I. Raskin, and B. Ensley, "Phytoremediation: a novel approach to an old problem," in *Studies in Environmental Science*, vol. 66, D. L. Wise, Ed. Elsevier, 1997, pp. 563–572. doi: 10.1016/S0166-1116(97)80071-4.

[41] B. E. Pivetz, *Phytoremediation of Contaminated Soil and Ground Water at Hazardous Waste Sites*. U.S. Environmental Protection Agency, Office of Research and Development, Office of Solid Waste and Emergency Response, 2001.

[42] L. Passatore, S. Rossetti, A. A. Juwarkar, and A. Massacci, "Phytoremediation and bioremediation of polychlorinated biphenyls (PCBs): State of knowledge and research perspectives," *J. Hazard. Mater.*, vol. 278, pp. 189–202, Aug. 2014, doi: 10.1016/j.jhazmat.2014.05.051.

[43] K. E. Gerhardt, X.-D. Huang, B. R. Glick, and B. M. Greenberg, "Phytoremediation and rhizoremediation of organic soil contaminants: Potential and challenges," *Plant Sci.*, vol. 176, no. 1, pp. 20–30, Jan. 2009, doi: 10.1016/j.plantsci.2008.09.014.

[44] X.-D. Huang, Y. El-Alawi, J. Gurska, B. R. Glick, and B. M. Greenberg, "A multi-process phytoremediation system for decontamination of persistent total petroleum hydrocarbons (TPHs) from soils," *Microchem. J.*, vol. 81, no. 1, pp. 139–147, Aug. 2005, doi: 10.1016/j.microc.2005.01.009.

[45] https://www.ehs.washington.edu/system/files/resources/literature-review-remediation-methods-pcbs.pdf (Accessed Dec. 26, 2021).

[46] M. Z. Velazco, P. G. V. Pedroso, G. V. Ramos, and H. V. Langehove, "Dehalogenation of Polychlorinated Biphenyls (PCBs) using chemical dechlorination," *Afinidad J. Chem. Eng. Theor. Appl. Chem.*, vol. 72, no. 571, Art. no. 571, Oct. 2015, Accessed: Dec. 31, 2022. [Online]. Available: https://raco.cat/index.php/afinidad/article/view/300885

[47] S. Xu, E. D'Angelo, D. Ghosh, J. Feliciano, S. K. Deo, and S. Daunert, "Detection of polychlorinated biphenyls employing chemical dechlorination followed by biphenyl whole cell sensing system," *Toxicol. Environ. Chem.*, vol. 87, no. 3, pp. 287–298, Jul. 2005, doi: 10.1080/02772240400029769.

[48] M. Vidali, "Bioremediation. An overview," *Pure Appl. Chem.*, vol. 73, no. 7, pp. 1163–1172, Jul. 2001, doi: 10.1351/pac200173071163.

[49] D. L. Bedard, "A case study for microbial biodegradation: anaerobic bacterial reductive dechlorination of polychlorinated biphenyls-from sediment to defined medium," *Annu. Rev. Microbiol.*, vol. 62, pp. 253–270, 2008, doi: 10.1146/annurev.micro.62.081307.162733.

[50] M. M. Häggblom, Y.-B. Ahn, D. E. Fennell, L. J. Kerkhof, and S.-K. Rhee, "Anaerobic Dehalogenation of Organohalide Contaminants in the Marine Environment," in *Advances in Applied Microbiology*, vol. 53, Academic Press, 2003, pp. 61–84. doi: 10.1016/S0065-2164(03)53002-7.

[51] J. A. Field and R. Sierra-Alvarez, "Microbial transformation and degradation of polychlorinated biphenyls," *Environ. Pollut.*, vol. 155, no. 1, pp. 1–12, Sep. 2008, doi: 10.1016/j.envpol.2007.10.016.

[52] "Polychlorinated Biphenyl Dechlorination in Aquatic Sediments." https://www.science.org/doi/10.1126/science.236.4802.709 (accessed Dec. 26, 2021).

[53] K. R. Sowers and H. D. May, "In situ treatment of PCBs by anaerobic microbial dechlorination in aquatic sediment: are we there yet?," *Curr. Opin. Biotechnol.*, vol. 24, no. 3, pp. 482–488, Jun. 2013, doi: 10.1016/j.copbio.2012.10.004.

[54] C. C. Azubuike, C. B. Chikere, and G. C. Okpokwasili, "Bioremediation techniques-classification based on site of application: principles, advantages, limitations and prospects," *World J. Microbiol. Biotechnol.*, vol. 32, no. 11, p. 180, Nov. 2016, doi: 10.1007/s11274-016-2137-x.

[55] J. K. Sharma *et al.*, "Advances and perspective in bioremediation of polychlorinated biphenyl-contaminated soils," *Environ. Sci. Pollut. Res.*, vol. 25, no. 17, pp. 16355–16375, Jun. 2018, doi: 10.1007/s11356-017-8995-4.

[56] https://hwbdocuments.env.nm.gov/Los%20Alamos%20National%20Labs/TA%2011/3654.pdf (Accessed Dec. 26, 2021).

[57] T. Held and H. Dörr, "In-Situ Remediation," in *Environmental Biotechnology*, John Wiley & Sons, Ltd, 2004, pp. 311–331. doi: 10.1002/3527604286.ch12.

[58] B. K. Gogoi, N. N. Dutta, P. Goswami, and T. R. Krishna Mohan, "A case study of bioremediation of petroleum-hydrocarbon contaminated soil at a crude oil spill site," *Adv. Environ. Res.*, vol. 7, no. 4, pp. 767–782, Jun. 2003, doi: 10.1016/S1093-0191(02)00029-1.

[59] "Dioxins sources and current remediation technologies — A review - ScienceDirect." https://www.sciencedirect.com/science/article/pii/S0160412007001390?casa_token=YffAoS8ny58AAAAA:hjxTiGDuIkkd7Yy5xkKU1hZK_NeOD_tROCPovKk2QcKfy-imR6uMR54Si-kwuRKA4Rx01CHleQ (accessed Dec. 26, 2021).

[60] P. C. Hung, W. C. Lo, K. H. Chi, S. H. Chang, and M. B. Chang, "Reduction of dioxin emission by a multi-layer reactor with bead-shaped activated carbon in simulated gas stream and real flue gas of a sinter plant," *Chemosphere*, vol. 82, no. 1, pp. 72–77, Jan. 2011, doi: 10.1016/j.chemosphere.2010.10.004.

[61] "In-Situ Chemical Oxidation." Accessed: Dec. 31, 2022. [Online]. Available: https://apps.dtic.mil/sti/citations/ADA507297

[62] Y. Mitoma *et al.*, "Approach to Highly Efficient Dechlorination of PCDDs, PCDFs, and Coplanar PCBs Using Metallic Calcium in Ethanol under Atmospheric Pressure at Room Temperature," *Environ. Sci. Technol.*, vol. 38, no. 4, pp. 1216–1220, Feb. 2004, doi: 10.1021/es034379b.

[63] K.-S. Ryoo *et al.*, "Destruction and Removal of PCBs in Waste Transformer Oil by a Chemical Dechlorination Process," *Bull. Korean Chem. Soc.*, vol. 28, no. 4, pp. 520–528, 2007, doi: 10.5012/bkcs.2007.28.4.520.

[64] I. W. Nah, K.-Y. Hwang, and Y.-G. Shul, "Effect of metal and glycol on mechanochemical dechlorination of polychlorinated biphenyls (PCBs)," *Chemosphere*, vol. 73, no. 1, pp. 138–141, Aug. 2008, doi: 10.1016/j.chemosphere.2008.04.051.

[65] J. Xu and D. Bhattacharyya, "Fe/Pd Nanoparticle Immobilization in Microfiltration Membrane Pores: Synthesis, Characterization, and Application in the Dechlorination of Polychlorinated Biphenyls," *Ind. Eng. Chem. Res.*, vol. 46, no. 8, pp. 2348–2359, Apr. 2007, doi: 10.1021/ie0611498.

[66] D. Crowley *et al.*, "Health and Environmental Effects of Landfilling and Incineration of Waste - A Literature Review," *Y Rep.*, Jan. 2003, [Online]. Available: https://arrow.tudublin.ie/schfsehrep/3

[67] B. Rahuman, L. Pistone, F. Trifirò, and S. Miertus, "Destruction technologies for polychlorinated biphenyls (PCBs)," vol. 7, May 2000.

[68] H.-K. Kim, J.-S. Chae, S.-S. Park, H.-S. An, K. Kim, and T.-I. Ohm, "Numerical simulations of the combustor for waste insulating oil containing polychlorinated biphenyls," *J. Mech. Sci. Technol.*, vol. 25, no. 7, p. 1853, Jul. 2011, doi: 10.1007/s12206-011-0428-6.

[69] E. H. Bani-Hani, M. Hammad, A. Matar, A. Sedaghat, and K. Khanafer, "Numerical analysis of the incineration of polychlorinated biphenyl wastes in rotary kilns," *J. Environ. Chem. Eng.*, vol. 4, no. 1, pp. 624–632, Mar. 2016, doi: 10.1016/j.jece.2015.12.006.

[70] V. Marulanda and G. Bolaños, "Supercritical water oxidation of a heavily PCB-contaminated mineral transformer oil: Laboratory-scale data and economic assessment," *J. Supercrit. Fluids*, vol. 54, no. 2, pp. 258–265, Aug. 2010, doi: 10.1016/j.supflu.2010.04.008.

[71] P. A. Marrone, M. Hodes, K. A. Smith, and J. W. Tester, "Salt precipitation and scale control in supercritical water oxidation—part B: commercial/full-

scale applications," *J. Supercrit. Fluids*, vol. 29, no. 3, pp. 289–312, May 2004, doi: 10.1016/S0896-8446(03)00092-5.

[72] H. I. Gomes, C. Dias-Ferreira, and A. B. Ribeiro, "Overview of in situ and ex situ remediation technologies for PCB-contaminated soils and sediments and obstacles for full-scale application," *Sci. Total Environ.*, vol. 445–446, pp. 237–260, Feb. 2013, doi: 10.1016/j.scitotenv.2012.11.098.

[73] B.-Z. Wu, H.-Y. Chen, S. J. Wang, C. M. Wai, W. Liao, and K. Chiu, "Reductive dechlorination for remediation of polychlorinated biphenyls," *Chemosphere*, vol. 88, no. 7, pp. 757–768, Aug. 2012, doi: 10.1016/j.chemosphere.2012.03.056.

[74] S. Agarwal, S. R. Al-Abed, and D. D. Dionysiou, "A feasibility study on Pd/Mg application in historically contaminated sediments and PCB spiked substrates," *J. Hazard. Mater.*, vol. 172, no. 2, pp. 1156–1162, Dec. 2009, doi: 10.1016/j.jhazmat.2009.07.117.

[75] M. Petruschke, "Tribochemistry. von G. HEINICKE. Berlin: Akademie-Verlag 1984. Bestellnummer: 7631993(6746). 495 S., 329 Bilder, 106 Tabellen, 98,– M," *Acta Polym.*, vol. 36, no. 7, pp. 400–401, 1985, doi: 10.1002/actp.1985.010360721.

[76] "International Union of Pure and Applied Chemistry." http://publications.iupac.org/compendium/index.html (accessed Dec. 18, 2022).

[77] C. Kajdas, E. Wilusz, and S. Harvey, *Encyclopedia of Tribology*. Elsevier, 1990.

[78] L. Takacs, "The mechanochemical reduction of AgCl with metals," *J. Therm. Anal. Calorim.*, vol. 90, no. 1, pp. 81–84, Oct. 2007, doi: 10.1007/s10973-007-8479-8.

[79] G. Kaupp, "Mechanochemistry: the varied applications of mechanical bond-breaking," *CrystEngComm*, vol. 11, no. 3, pp. 388–403, Feb. 2009, doi: 10.1039/B810822F.

[80] L. Takacs, "The historical development of mechanochemistry," *Chem. Soc. Rev.*, vol. 42, no. 18, pp. 7649–7659, Aug. 2013, doi: 10.1039/C2CS35442J.

[81] X. Guo, D. Xiang, G. Duan, and P. Mou, "A review of mechanochemistry applications in waste management," *Waste Manag.*, vol. 30, no. 1, pp. 4–10, Jan. 2010, doi: 10.1016/j.wasman.2009.08.017.

[82] L. Takacs, "What Is Unique About Mechanochemical Reactions?," *Acta Phys. Pol. A*, vol. 4, no. 126, pp. 1040–1043, 2014, doi: 10.12693/APhysPolA.126.1040.

[83] M. Monagheddu, G. Mulas, S. Doppiu, G. Cocco, and S. Raccanelli, "Reduction of Polychlorinated Dibenzodioxins and Dibenzofurans in Contaminated Muds by Mechanically Induced Combustion Reactions," *Environ. Sci. Technol.*, vol. 33, no. 14, pp. 2485–2488, Jul. 1999, doi: 10.1021/es9809206.

[84] A. Stolle, T. Szuppa, S. E. S. Leonhardt, and B. Ondruschka, "Ball milling in organic synthesis: solutions and challenges," *Chem. Soc. Rev.*, vol. 40, no. 5, pp. 2317–2329, Apr. 2011, doi: 10.1039/C0CS00195C.

[85] G. R. Gossweiler *et al.*, "Mechanochemical Activation of Covalent Bonds in Polymers with Full and Repeatable Macroscopic Shape Recovery," *ACS Publications*, Feb. 12, 2014. https://pubs.acs.org/doi/pdf/10.1021/mz500031q (accessed Dec. 17, 2022).

[86] P. Baláž, A. Aláčová, M. Achimovičová, J. Ficeriová, and E. Godočíková, "Mechanochemistry in hydrometallurgy of sulphide minerals," *Hydrometallurgy*, vol. 77, no. 1, pp. 9–17, Apr. 2005, doi: 10.1016/j.hydromet.2004.09.009.

[87] M. Aresta, P. Caramuscio, L. De Stefano, and T. Pastore, "Solid state dehalogenation of PCBs in contaminated soil using NaBH4," *Waste Manag.*,

vol. 23, no. 4, pp. 315–319, Jan. 2003, doi: 10.1016/S0956-053X(03)00029-1.

[88] B. Bhushan, Ed., "Fundamentals of Tribology and Bridging the Gap Between the Macro- and Micro/Nanoscales," Dordrecht, 2001. doi: 10.1007/978-94-010-0736-8.

[89] V. Birke, J. Mattik, D. Runne, H. Benning, and D. Zlatovic, "Dechlorination of Recalcitrant Polychlorinated Contaminants Using Ball Milling," in *Ecological Risks Associated with the Destruction of Chemical Weapons*, Dordrecht, 2006, pp. 111–127. doi: 10.1007/1-4020-3137-8_13.

[90] P. Donecker, P. G. Mccormick, R. Street, and S.-A. Rowlands, "Toxic material disposal," CA2152081A1, Jul. 07, 1994 Accessed: Jun. 20, 2022. [Online]. Available: https://patents.google.com/patent/CA2152081A1/en

[91] Y. Tanaka, Q. Zhang, and F. Saito, "Mechanochemical Dechlorination of Trichlorobenzene on Oxide Surfaces," *J. Phys. Chem. B*, vol. 107, no. 40, pp. 11091–11097, Oct. 2003, doi: 10.1021/jp0276808.

[92] H. Wang *et al.*, "Mechanochemical remediation of PCB contaminated soil," *Chemosphere*, vol. 168, pp. 333–340, Feb. 2017, doi: 10.1016/j.chemosphere.2016.10.073.

[93] V. Birke, J. Mattik, and D. Runne, "Mechanochemical reductive dehalogenation of hazardous polyhalogenated contaminants," *J. Mater. Sci.*, vol. 39, no. 16, pp. 5111–5116, Aug. 2004, doi: 10.1023/B:JMSC.0000039192.61817.dd.

[94] V. V. Boldyrev and K. Tkáčová, "Mechanochemistry of Solids: Past, Present, and Prospects," *J. Mater. Synth. Process.*, vol. 8, no. 3, pp. 121–132, Jul. 2000, doi: 10.1023/A:1011347706721.

[95] J. L. Nelson, J. Jiang, and S. H. Zinder, "Dehalogenation of Chlorobenzenes, Dichlorotoluenes, and Tetrachloroethene by Three Dehalobacter spp.," *Environ. Sci. Technol.*, vol. 48, no. 7, pp. 3776–3782, Apr. 2014, doi: 10.1021/es4044769.

[96] P. Fürst, C. Krüger, H.-A. Meemken, and W. Groebel, "Determination of the polychlorinated biphenyl substitute ugilec (tetrachlorobenzyltoluenes) in fish," *J. Chromatogr. A*, vol. 405, pp. 311–317, Jan. 1987, doi: 10.1016/S0021-9673(01)81772-6.

[97] "3,4-Dichlorotoluene 97 95-75-0." http://www.sigmaaldrich.com/ (accessed Dec. 25, 2021).

[98] "Hexadecane ReagentPlus , 99 544-76-3." http://www.sigmaaldrich.com/ (accessed Dec. 25, 2021).

[99] J. He, "ASTM 52100 Bearing Steel | 100Cr6 | SUJ2 | EN31," *Otai Special Steel*. https://www.astmsteel.com/product/52100-bearing-steel-aisi/ (accessed Dec. 24, 2021).

[100] D. A. Kramer, "Magnesium recycling in the United States in 1998," USGS Numbered Series 1196-E, 2002. doi: 10.3133/cir1196E.

[101] Y. Hu, D. Dong, X. Wang, H. Chen, and Y. Qiao, "Synthesis and Properties of Mg-Mn-Zn Alloys for Medical Applications," *Materials*, vol. 14, no. 8, Art. no. 8, Jan. 2021, doi: 10.3390/ma14081855.

[102] "Influence of Dielectric Type on Porosity Formation on Electrical Discharge Machined Surfaces | SpringerLink." https://link.springer.com/article/10.1007%2Fs11663-012-9653-3 (accessed Dec. 24, 2021).

[103] P. Burke, G. J. Kipouros, D. Fancelli, and V. Laverdiere, "Sintering Fundamentals of Magnesium Powders," *Can. Metall. Q.*, vol. 48, no. 2, pp. 123–132, Jun. 2009, doi: 10.1179/cmq.2009.48.2.123.

[104] J. W. H. Murray, "Damage, contamination and surface treatment of electrical discharge machined materials," Jul. 09, 2014. http://eprints.nottingham.ac.uk/14226/ (accessed Dec. 24, 2021).

[105]   "Infrared Spectroscopy Absorption Table," *Chemistry LibreTexts*, Nov.   30,   2014. https://chem.libretexts.org/Ancillary_Materials/Reference/Reference_Tables/ Spectroscopic_Parameters/Infrared_Spectroscopy_Absorption_Table (accessed May 23, 2021).

[106]   "Infrared: Interpretation," *Chemistry LibreTexts*, Oct. 02, 2013. https://chem.libretexts.org/Bookshelves/Physical_and_Theoretical_Chemistr y_Textbook_Maps/Supplemental_Modules_(Physical_and_Theoretical_Che mistry)/Spectroscopy/Vibrational_Spectroscopy/Infrared_Spectroscopy/Infra red%3A_Interpretation (accessed May 23, 2021).

[107]   "Equipment," *CIC nanoGUNE*. https://www.nanogune.eu/en/nanogune/glance/facilities-equipment/equipment (accessed Dec. 24, 2021).

[108]   T. Theophanides, "Introduction to Infrared Spectroscopy," 2012. doi: 10.5772/49106.

[109]   J. Cejka, *Zeolites and Ordered Mesoporous Materials: Progress and Prospects: The 1st FEZA School on Zeolites, Prague, Czech Republic, August 20-21, 2005*. Elsevier, 2005.

[110]   B. E. P. Di, "Process for the production of 2, 4-dichlorotoluene," US3366698A, Jan. 30, 1968 Accessed: Jun. 24, 2022. [Online]. Available: https://patents.google.com/patent/US3366698A/en